Development of Structural Lightweight Aggregate Concrete by Coarse Rigid Polyurethane Foam Waste

FINAL YEAR PROJECT UG 2018

By

Muhammad Mahmood Mohi Ud Din	00000 269191
Muhammad Ovais Hafeez	00000 255080
Usama Shahbaz Cheema	00000 264215
Muhammad Husnain Arshad	00000 271287

NUST Institute of Civil Engineering (NICE)
School of Civil and Environmental Engineering (SCEE)
National University of Science and Technology (NUST), Islamabad, Pakistan

2022

This is to certify that the Final Year Project Titled

"Development of Structural Lightweight Aggregate Concrete by Coarse Rigid Polyurethane Foam Waste"

Submitted By

Muhammad Mahmood Mohi Ud Din	00000 269191
Muhammad Ovais Hafeez	00000 255080
Usama Shahbaz Cheema	00000 264215
Muhammad Husnain Arshad	00000 271287

has been accepted towards the requirements for the undergraduate degree

in

CIVIL ENGINEERING

Dr. Musaad Zaheer Nazir Khan
Assistant Professor
NUST Institute of Civil Engineering
School of Civil and Environmental Engineering
National University of Sciences and Technology, Islamabad, Pakistan

DEDICATION

To our beloved parents, teachers, mentors, and colleagues who have stood by our side in rough and tough times, who have taught us to show perseverance in the face of adversity.

ACKNOWLEDGEMENTS

In the name of Allah, the most Beneficent, the most Merciful as well as peace and blessings upon Prophet Muhammad, His servant and final messenger.

First of all, we would like to thank our Creator Allah the Almighty, who has blessed us with the opportunity to perform this research. His guidance through each and every adversity while carrying out our research work, is what has led us to complete and compile our work in time.

We are also greatly thankful to our parents who have supported us through every thick and thin of our life's journey. They have supported us when we were not able to walk, and they are still supporting us to continue and provide solutions for humanity.

We are also obliged from the depths of our hearts to pay special thanks to our supervisor, Dr. Musaad Zaheer Nazir Khan. His guidance throughout the project has been a great learning experience for us and the knowledge he has imparted in us will be one the primary factors for our growth. He has also helped us in every part of our thesis and above all, he was always there to guide us and was our constant support and motivator throughout the project. We feel the responsibility to thank him for his patience, guidance, and cooperation throughout our final year project.

We are also extremely grateful to and value the assistance provided by Mr. Mati Ullah Shah and the entire staff of Structures Lab at NICE. They have been a vital element to our success and have helped us conduct experiments and procure materials and equipment.

Finally, I, Muhammad Mahmood Mohi Ud Din, the group leader for this project, would like to pay my sincerest gratitude to my dear group members, who took matters into hand, followed my guidance by heart, sacrificed their sleep and carried out experimental work in scorching heat despite fasting, when time of adversity came upon me. Lastly, we as a group, would like to pay our gratitude to anyone and everyone, who participated knowing and unknowingly, to assist us in our endeavors while carrying out this study.

ABSTRACT

The aim of this thesis was to research and develop a structural lightweight concrete by incorporation of rigid polyurethane foam waste as coarse aggregates (5-10 mm), which would offer a solution for eco-friendly and economical construction in Pakistan. In this regard, the first phase of the project aimed at optimizing a suitable concrete mix design and promote sustainability by integration of Polyurethane Foam Waste and Silica Fume, which are potential indigenous wastes. Silica Fume was incorporated as a cement replacement at 0,5,10,15 and 20% by weight of cement. Three mix formulations consisting of polyurethane foam, cement coated polyurethane foam and pumice as coarse aggregates were tested for workability, compressive strength, flexural strength, elastic modulus, absorption, permeable voids, chloride-ion penetration, and drying shrinkage. Pumice based Lightweight concrete was manufactured as control mix for comparison. The results revealed that uncoated polyurethane based lightweight aggregate concrete yielded an air-dry density of 1829 kg/m^3 with the corresponding compressive strength of 19.5 MPa and flexural strength of 2.78 MPa at 28 days, in addition to satisfying the criteria for elastic modulus, chloride ion penetrability and drying shrinkage, making the lightweight concrete suitable for structural use. Maximum mechanical strengths were achieved at 10% cement replacement by silica fume. The second phase of this project consisted of analyzing the durability and thermal properties of lightweight aggregate concrete, by testing the samples in freeze and thaw action. Polyurethane-based lightweight concrete demonstrated less internal structure damage against freeze and thaw action. In addition, the thermal conductivity value of the samples was evaluated using thermal conductivity meter and the average thermal conductivity value (K-value) was found out to be 0.371 W/m.k. Scanning Electron Microscope (SEM) analysis was conducted to study the interfacial transition zone and analyze the elemental percentages. Elemental data was comparable in both polyurethane-based concrete and pumice-based concrete. It is believed that utilizing these “low cost” lightweight aggregate helps to lower the cost per unit volume of lightweight aggregate concrete.

Key words: Polyurethane foam, structural lightweight concrete, shrinkage, pumice

TABLE OF CONTENTS

LIST OF FIGURES

LIST OF TABLES

CHAPTER 1: INTRODUCTION

1.1 General

The compressive strength of concrete is an important factor in determining the concrete quality, besides the durability at the service stage. As a matter of fact, most of the reinforced concrete structures building codes suggested design guidelines are based on this property. However, the advancement in technology poses a great challenge to humanity to explore different methods and means to improve concrete as a material. One such method is to adopt the use of lightweight concrete. Lightweight concrete has been widely used in countries including the United States, the United Kingdom, and Sweden [1]. It is because the reduced concrete density leads to more cost-effective construction as it lowers the cost of transportation, handling, and constructability [2]. Shale, pumice, perlite, and other lightweight aggregate are combined with an air-entraining agent to lighten the concrete. Construction time, dead load, and haulage and handling expenses can all be decreased by using lightweight aggregate and an air entraining agent. The emergence of LWC gives the building industry, which is now centered on natural resources, new possibilities even if the application of LWC (Lightweight Concrete) is restricted to certain tasks when compared to ordinary concrete.

Pakistan is a region of diverse climatic conditions due to which reinforced concrete buildings face various issues mainly related to insulation in hot regions, freezing and thawing in cold regions etc. The conventional concrete is not capable of solving all these issues, but with the properties the lightweight aggregate offers, this issue can be resolved. For example, Perlite is frequently used as loose-fill insulation in brick building because of its exceptional insulating properties. This insulation improves fire ratings, lessens noise transmission, doesn't decay, and is termite resistant [1]

1.2 Research Significance

The production and utilization of LWAC (Lightweight Aggregate Concrete) is significant for building and maintenance of construction works. Researchers all over the world are focusing on lightweight concrete because it can increase the affordability and toughness of structural systems. Polyurethane is a cost-effective and environmentally friendly waste product that can be found all over the world. However, in lightweight concrete, the performance of polyurethane is relatively unknown or little investigated. The current investigation is focused on determining the density, mechanical characteristics,

drying shrinkage, freeze and thaw resistance, electrical resistivity, and thermal conductivity of polyurethane-based concrete with consideration for structural application.

1.3 Polyurethane Foam

Among the most significant polymer product categories within the plastics family is polyurethane. Early in the twenty-first century, PUR (Polyurethane) usage in Europe is predicted to reach approximately 3 million tons annually. It comprises of several goods, including 0.4 million tons of Polyurethane elastomer, around 1.8 million tons of flexible Polyurethane foam and 0.7 million tons of rigid Polyurethane foam [3]. PUR is a waste product and is mainly generated during fabrication and conditioning. To address this issue, recycling and particular valorization techniques must be created [4].

One way of recycling PU is by incorporating it in concrete in rigid form. PU belongs in the category of lightweight aggregate as PU sheets density ranges from 30 to 50 kg/m^3. It can either be incorporated in concrete in spray form or rigid form. Addition of PU as a complete or partial replacement of coarse aggregate will greatly reduce the dead load of concrete due to its extremely low density. Polyurethane offers various benefits when compared to conventional aggregate. These benefits include, reduced self-weight as compared to gravel, good thermal insulation, and reduction in reliance of heavy equipment and machinery for the transportations and construction of structures on site when compared to regular pre-cast concrete structures. Due to its exceptional qualities and morphology, PU is regarded as a versatile material and has an ability to modify its microstructure while obtaining several mechanical qualities, including stiffness or elasticity, flexibility, and excellent damping capabilities, as well as durability to shock, abrasion, and weather [5,6]. It is formed by the chemical reaction between Polyol and Isocyanate as shown below in Figure 1.

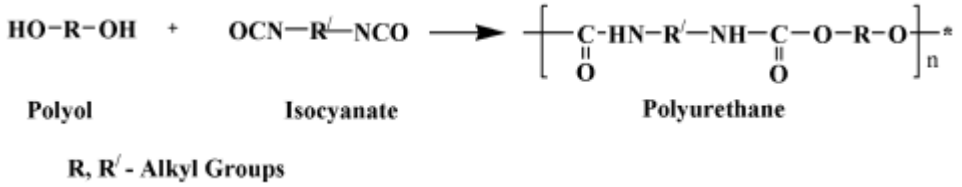

Figure 1: The chemical composition of Polyurethane

1.4 Incorporation of SF (Silica Fume)

SF is a widely used additive in concrete due to its pozzolanic qualities. It is a by-product of silicon metal production. Amorphous silica fibers that are typically 10–15 μm long, with diameters ranging from 0.5–1 μm make up silica fume. It also contains small amounts (0.5%) of aluminum oxide and iron oxide particles, which can act as nucleation sites for calcium hydroxide ($Ca(OH)_2$) formation during hydration reactions [7].

Silica fume use in concrete is still a subject of debate, but it has been proven to be an efficient additive. It is added as a percentage substitute for cement. Concrete's strength and durability are both increased with the addition of SF [8]. When added as a dry powder (up to 10 percent by weight), the cement paste's hydration temperature is raised with silica fume, allowing more time for water to react with lime (CaO). This results in higher-strength concrete with less cracking and lower permeability [9].

1.5 Thesis Objectives

The salient objectives of this research were to:

1) To investigate the reuse of Polyurethane foam waste in concrete.
2) To study the mechanical properties of PU-based LWC such as elastic modulus, compressive and flexural strength as well as shrinkage properties.
3) To optimize the binder/cement ratio and percentage of additives (SF and Superplasticizer) to achieve the maximum strength.
4) To compare the mechanical properties of PU based concrete with pumice-based concrete
5) To develop structural lightweight concrete building material with good thermal insulation and freeze/thaw resistance.

CHAPTER 2: LITERATURE REVIEW

2.1 Polyurethane based Lightweight concrete

In the past, several studies and experiments have been conducted in which the researchers have used polyurethane in concrete. A lot of study has been conducted on Polyurethane foam used as an insulating layer on concrete. Previous research demonstrates the structural and non-structural uses of PU-based concrete. In the last few decades, its variations have developed into a popular and efficient technology for repairing, reinforcing, rehabilitating, and protecting buildings. Some researchers have partially replaced coarse aggregate with Polyurethane Foam while some have completely replaced coarse aggregate with Polyurethane Foam to make structural as well as non-structural Lightweight concrete.

Firyal Mohammed Ali et al. conducted an experiment in which they added PU as a coarse aggregate and focused on the performance of LWC related to the compressive strength, density, thermal conductivity, and water absorption test of different test mixes [10]. They achieved a strength greater than 3.45 MPa making it suitable as a non-load bearing structure. It was observed that the crushed PU concrete has lesser workability than that of normal concrete which increases the water absorption of concrete [10].

Vojtěch Václavík et al. [11] conducted an experiment in which they varied the density from 400 to 1200 kg/m^3. They achieved the compressive strength ranging from 0.6 to 5.1 MPa and recommended that this Polyurethane material is suitable for floors, terraces, sound insulation panels and prefabricated products.

Amor Ben Fraj et al. conducted a study to determine the mechanical characteristics and durability parameters of Polyurethane based LWC in which he replaced PU with coarse aggregate – size 8/20 mm [12]. They investigated and analyzed the influence on the workability, bulk density, loss of mass, drying shrinkage, compressive strength, dynamic elastic modulus, total porosity, etc. by increasing the amount of PU foam and addition of superplasticizer. They prepared different samples, one with simple Polyurethane Foam and the other with saturated Polyurethane Foam. The dynamic elastic modulus ranged from 10 to 15 GPa, and the compressive strength ranged from 8 to 16 MPa [12]. The results met the requirements for structural lightweight concrete.

P. Mounanga et al. conducted experiments incorporating Polyurethane waste into cementitious mixtures in different fractions [4]. PU foam is highly compressible and has high absorption rate, therefore it was difficult to estimate the density of PU foam.

Density was found to be 25 – 63 % lesser than the normal/reference material. In comparison to the reference material, the thermal conductivity is 2 to 7 times and compressive strength is 2 to 17 times lower. This was mostly caused by the high porosity of the LWA (Lightweight Aggregate) . The use of Polyurethane as an aggregate also implies a significant rise in the drying shrinkage and mass loss during the first 7 days [4].

Iman Kattoof Harith carried out a study by experimenting with different curing techniques which examined the feasibility of producing foamed concrete as a sustainable structural material [13]. Her study has shown potential for using Polyurethane based concrete as a structural member. The results also showed that moisture curing is the most suitable method as the highest compressive strength at all ages was achieved with it compared to rest of the curing methods [13].

2.2 Impact of SF in Concrete

K. Ganesh Babu et al. conducted research in which they examined the durability and mechanical strength of Expanded Polystyrene concretes with the addition of silica fumes added in it at varying percentages [14]. Different samples had varying densities with strength also varying from 10 to 21 MPa making it suitable to be used as a structural member since some samples with specific amount of silica content exceeded the strength limit of 17 MPa i.e., the minimal requirement of structural concrete. The experiment showed that by increasing silica content, the 7-day strength of EPS concrete also increases. At the SF (silica fume) replacement levels of 3%, 5%, and 9%, this was found to be approximately 75%, 85%, and 95% of the corresponding 28-day strength, respectively. Addition of silica fume also resulted in decrease in the absorption of EPS concretes. As compared to normal concrete, silica-containing EPS concretes had much lower corrosion rate and low chloride ion permeability i.e., of less than 1000 C [14].

V.T. Giner et al. added silica fumes at varying percentages in concrete to study the affect silica fumes have on the dynamic and static mechanical properties of concrete [15]. Multiple conclusions were made based on their research. Increase in silica fume results in slight reduction in the resonant frequency and dynamic elastic modulus of the concrete. The compressive strength increases proportionally with increasing amount of silica fume added [15].

N. K. Amudhavalli et al. also proved with their research that SF increases the concrete's strength [16]. They substituted cement partially with 0, 5, 10, 15 and 20 % silica fume and

carried out a comprehensive experimental investigation on the compressive, split tensile and flexural strength of concrete at ages of 7 and 28 days. The ratio of cement to SF replacement, which ranged from 10 to 15 percent, resulted in the best 7 and 28 day compressive and flexural strength. Flexural strength of concrete was significantly impacted by the addition of SF, as compared to the split tensile strength of concrete [16].

H. Katkhuda et al. conducted detailed experiment to investigate the effects of partially replacing cement with silica fumes with varying w/c ratios [17]. Optimum water to cement ratio and SF amount was determined by comparing concrete samples of varying percentage of silica fume and w/c ratios. The split tensile, compressive, and flexural strengths of SF concrete were correlated using statistical techniques based on the findings [17].

Dilip Kumar Singha Roy et al. conducted an experimental study that concluded that silica fume is beneficial for both high early and low/medium strength concrete [18]. It is due to the fact that silica fume facilitates the use of less water in the cement mix, which results in better cement particles hydration and stronger bonding between them. When silica fume was used to replace 10% of the cement, remarkable increase in compressive, flexural, and tensile strength was observed compared to normal concrete. With some appropriate level of quality control, Silica fume concrete can be utilized in situations where chemical attack, frost action, and other factors may occur since it is more compact and so more robust in nature [18].

CHAPTER 3: EXPERIMENTAL PROGRAM, MATERIALS AND METHOLODY

3.1 Mix Formulations

This research was based on three different aggregates namely PU Foam (A), Coated PU (B) and Pumice (C), each incorporated with different percentages of silica fume. These mix formulations included complete replacement of Normal aggregate with uncoated PU foam aggregates (A), Coated PU foam aggregates (B) and Pumice aggregates (C). So, a total of 15 mix formulations were prepared i.e., 5 mix designs for each lightweight aggregate concrete were prepared. It includes one control mix without silica fume and the remaining mixes with silica fume added to substitute cement by 5, 10, 15 and 20 %. In addition, Bond Rheoplast 250 Superplasticizer was added by 1.1 % of the weight of the binder to lower the water requirement and it help to improve the strength of the binder by maintaining a steady flow. The value of water/cement ratio and superplasticizer were optimized by Trial and error in the initial stages of the research. Samples with different water/binder ratios and percentage of superplasticizer were tested in compression which helped us optimize the water/binder ratio to 0.45 and superplasticizer as 1.1 % of cement. The mix formulations are shown in Table 1.

Table 1: Mix formulations

Serial	Formulations	Cement (kg/m^3)	Sand (kg/m^3)	PU (kg/m^3)	Pumice (kg/m^3)
1.	0A	493	992	8.5	-
2.	5A	468.3	992	8.5	-
3.	10A	443.7	992	8.5	-
4.	15A	419	992	8.5	-
5.	20A	394.4	992	8.5	-
6.	0B	493	992	219.8	-
7.	5B	468.3	992	219.8	-
8.	10B	443.7	992	219.8	-
9.	15B	419	992	219.8	-
10.	20B	394.4	992	219.8	-
11.	0C	493	992	-	236.8
12.	5C	468.3	992	-	236.8
13.	10C	443.7	992	-	236.8
14.	15C	419	992	-	236.8
15.	20C	394.4	992	-	236.8

Serial	Formulations	Water (kg/m^3)	Silica Fume (kg/m^3)	Superplasticizer (kg/m^3)
1.	0A	216.6	0	5.4
2.	5A	216.6	24.7	5.4
3.	10A	216.6	49.3	5.4
4.	15A	216.6	74	5.4
5.	20A	216.6	98.6	5.4
6.	0B	216.6	0	5.4
7.	5B	216.6	24.7	5.4
8.	10B	216.6	49.3	5.4
9.	15B	216.6	74	5.4
10.	20B	216.6	98.6	5.4
11.	0C	216.6	0	5.4
12.	5C	216.6	24.7	5.4
13.	10C	216.6	49.3	5.4
14.	15C	216.6	74	5.4
15.	20C	216.6	98.6	5.4

3.2 Experimental Program for Casting Cylinders

A total of 225 cylindrical specimens were casted in the experimental program. The dimension of the cylinders was 100mm by 200mm. In addition, 12 beams were casted for flexural test, 4 for each A, B and C. The dimensions of the beam were 100 mm by 100 mm by 400 mm. Total samples casted for different tests are shown below in Table 2. Table 3 depicts the dimensions of samples for different tests.

Table 2: Samples casted for Testing

Tests	Pumice Samples	PU Samples	Coated PU Samples	Total Samples
Compressive Strength	30	30	30	90
Flexural Strength	4	4	4	12
Slump	4	4	4	12
Drying Shrinkage	2	2	2	6
Electrical Resistivity	5	5	5	15
Modulus of Elasticity	30	30	30	90
Thermal Conductivity	3	3	3	9
Frost Resistance	5	5	5	15

Table 3: Dimensions of moulds

Tests	Moulds
Compressive Strength	100mm x 200mm cylinders
Flexural Strength	100mm x 100mm x 400mm Prisms
Slump	Slump cone
Drying Shrinkage	25mm x 25mm x 285mm Prisms
Electrical Resistivity	100mm x 200mm Cylinders
Modulus of Elasticity	100mm x 200mm Cylinders
Thermal Conductivity	50mm x 25mm Disc
Freeze-Thaw Resistance	50mm x 50mm x 50mm sawn slab

3.3 Materials

3.3.1 Cement

Bestway Cement, which is an OPC (Ordinary Portland Cement), complies with ASTM C 150 [19] was utilized. Table 4 summarizes the chemical composition of cement and SF, and Table 5 summarizes the physical properties of Cement and SF**.** The cement had a specific gravity of around 3.15.

Table 4: Cement and Silica Fume's chemical composition

Sr. No	Chemical Composition	Cement (% by Weight)	SF (% by Weight)
1.	SiO_2	19.84	87.01
2.	Al_2O_3	4.35	0.00
3.	Fe_2O_3	3.63	2.44
4.	CaO	62.72	1.72
5.	MgO	2.68	0.8
6.	K_2O	0.83	0.79
7.	Na_2O	0.17	0.88
8.	SO_3	2.82	0.39
9.	Cl	0.001	0.095

Table 5: Physical composition of cement and SF

Sr. No	Physical Property	Cement	Silica Fume
1.	Appearance	Greyish Powder	Grey Powder
2.	Specific Gravity	3.15	2.2
3.	Normal Consistency (%)	26	N/A
4.	Blaine Fineness (cm2/gm)	3650	-
5.	Mean Particle Size	-	0.5 um
6.	Location	Bestway Cement	Imporient Chemicals Pvt. ltd.
7.	IST (Initial Setting Time) (min)	100	-
8.	FST (Final Setting Time) (min)	170	-

3.3.2 SF (Silica Fume)

SF utilized in our research was procured from Imporient Chemicals Pvt. Ltd., which is located in Lahore. X-Ray Fluorescence (XRF) spectrometer was used by Bestway Cement Limited to conduct the XRF Analysis of the sample to ascertain the chemical composition of silica fume. Table 4 and 5 depicts the chemical composition and physical properties of the sample, confirming to ASTM C 1240–05 [20].

According to ASTM C 1240-05, minimum percentage of SiO_2 required is 85 % [20]. The Silica Fume which was used has SiO_2 of 87.01 percent which is greater than the minimum requirement.

3.3.3 Admixture

Superplasticizer Bond Rheoplast-250, a specialized formulation of synthetic polymers, was used in the current study. The sample was in aqueous form and conformed to the ASTM C494-08 standards [21]. Table 6 depicts the admixture properties that was used in the study.

Table 6: Bond Rheoplast 250 superplasticizer properties

Serial	Parameter	Property
1.	Form	Liquid
2.	Color	Black Liquid
3.	Specific Gravity	1.21 g/cm^3
4.	Water Reduction	≥ 112% of Reference mix
5.	Shelf Life	12 months
6.	Max. Dosage (by mass of binder)	0.8-2%

3.3.4 Fine Aggregate

Lawrencepur sand was procured to be utilized as fine aggregate. According to ASTM C 136-04 [22] a sieve analysis was conducted to ascertain the properties of sand. The results were compared with the requirements set by ASTM C33-07 [23] and are presented in Table 7. Table 8 summarizes the physical properties of the fine aggregate.

Table 7: Fine Aggregate-Sieve Analysis Results

Sieve # (ASTM)	Cumulative Mass Retained (gm)	Cumulative % Age Retained (%)	Cumulative finer Percentage (%)	Range ASTM C-33
#4	7	1.26	98.74	95-100
#10	23	4.14	95.86	80-100
#16	95	17.12	82.88	50-85
#30	229	41.26	58.74	25-60
#40	384	69.19	30.81	10-50
#50	486	87.57	12.43	5-30
#100	542	97.66	2.34	2-10
#200	555	100	0	0-7

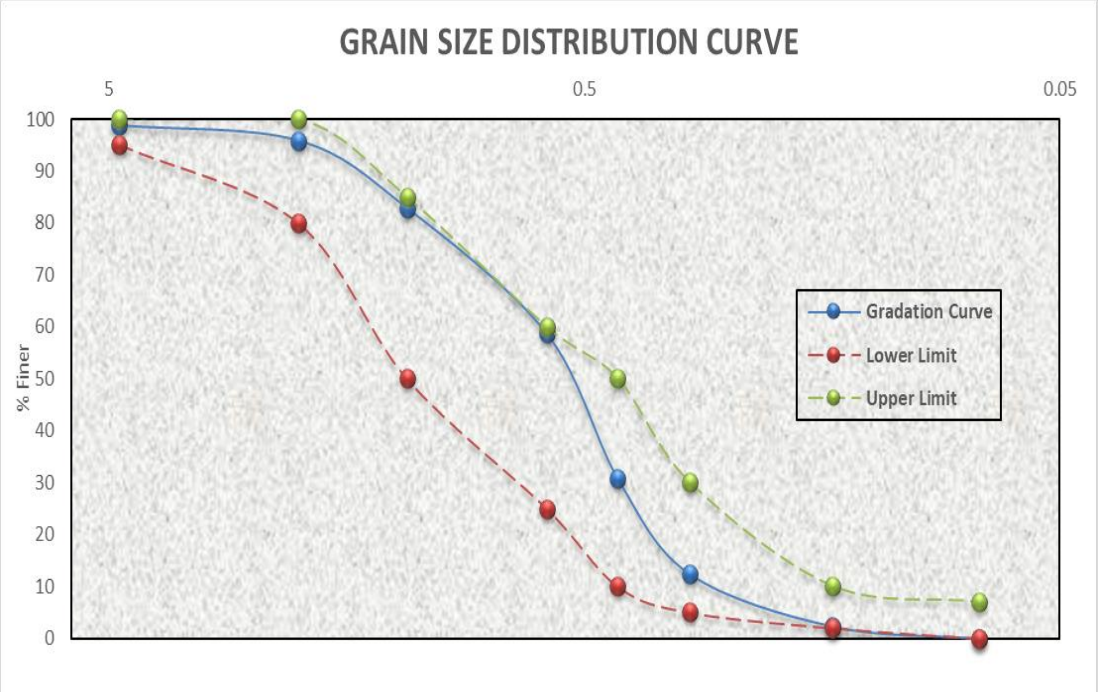

Figure 2: Results of Sieve Analysis

Table 8: Fine Aggregates-Physical Properties

Serial	Parameter	Results
i.	Fineness Modulus	2.98
ii.	O.D Bulk Specific Gravity	2.69
iii.	S.S.D Bulk S.G (Specific Gravity)	2.70
iv.	D50 (mm)	0.55
v.	Absorption (%)	1.6%
vi.	Quarry	Lawrencp ur Sand

3.3.5 Polyurethane (PU) Foam

Normal weight coarse aggregates were fully replaced by polyurethane foam and pumice aggregates. PU sheets have extremely low density of 40 ± 10 kg/m^3. Table 9 shows the material properties of Polyurethane foam sheets.

Table 9: Polyurethane Foam-Material Properties

Serial	Parameter	Value
1.	Nominal Density	40 ± 10 kg/m^3
2.	Thermal Conductivity	0.033 W/m.K
3.	Diameter	5 – 12 mm
4.	O.D Bulk Specific Gravity	0.83
5.	S.S.D Bulk Specific Gravity	1.01
6.	Absorption	21.5 %

(a) (b)

Figure 3: (a) Polyurethane foam Sheets (b) PU sheets broken into aggregates

3.3.6 Cement Coated Polyurethane

Coated Polyurethane aggregates are prepared by mixing PU Foam with cement slurry as shown in Figure 4. After coating PU with cement, it was air dried for 1.5 hours in order to strengthen the coating. This resulted in increase in density and decrease in absorption of polyurethane aggregates. The material properties of cement coated polyurethane are tabulated in Table 10.

Table 10: Material Properties of Cement Coated Polyurethane

Serial	Parameter	Value
1.	Nominal Density	325 ± 10 kg/m^3
2.	Absorption	9 %
3.	Diameter	5 – 12 mm
4.	O.D Bulk Specific Gravity	0.98
5.	S.S.D Bulk Specific Gravity	1.06

Figure 4: Cement coated PU foam aggregates

3.3.7 Pumice aggregate

Pumice is a conventional lightweight aggregate as shown in Figure 5, which was used as a control sample in this research. It was incorporated by completely replacing coarse aggregate with it in concrete specimens. The material properties of pumice are detailed in Table 11.

Table 11: Pumice Stone-Material Properties

Serial	Parameter	Value
1.	Nominal Density	420 ± 10 kg/m^3
2.	Thermal Conductivity	0.433 W/m.K
3.	Diameter	6 – 12 mm
4.	O.D Bulk Specific Gravity	0.86
5.	S.S.D Bulk Specific Gravity	1.04
6.	Absorption	20.5 %

Figure 5: Pumice Stone

3.4 Mixing Regime, Casting and Curing

3.4.1 Mixing Regime

The standard ASTM C192-02 [24] has been adopted for the mixing regime and all samples were prepared with the same uniformity in a 108 L capacity Pan mixer. At first, the required quantities, which were calculated while designing the mix formulations, were measured using the weight balance machine in the Structures Lab. After measuring the quantities, they were fed into the Pan mixer, followed by addition of required amount of water and Superplasticizer (SP). At first, only half amount of water was added and was allowed to mix for 2 minutes. After 2 minutes, the mixer was stopped for 15 seconds to scrape off the paste material adhered to the side surface of the mixer. The mixer was started again and the remaining water along with SP was added in the concrete mix. After 5 minutes, the mixer was stopped, and the batch was removed from it. The fresh mixture was immediately poured into molds of different sizes and shapes

needed for different tests: 100mm by 200mm cylinders and 100mm by 100mm by 400mm prisms. Mechanical Vibrator was used for compaction of cylinders and beams. The samples were left to harden for 24 hours in the casting room at room temperature and later placed under jute bags for moisture curing.

In the case of cement coated polyurethane aggregates, polyurethane foam aggregates were first mixed with cement slurry and left to dry for half an hour. After this, same mixing procedure was carried out as mentioned above.

3.4.2 Casting of samples

A total of 225 cylinders and 12 beams were casted for different tests. Cylinders were casted for Compression, Modulus of Elasticity and Electrical Resistivity as shown in Figure 6 (a). Beams were casted for Flexural Testing. Capping was applied on both sides of cylinder by using Plaster of Paris for testing in compression as shown in Figure 6 (b). Number of samples casted for each experiment are already tabulated in Table 2 and their shape as well as dimensions are detailed in Table 3.

(a) (b)

Figure 6: (a) Casted Cylinders (b) Capped Cylinders

3.4.3 Curing of samples

From the previous studies, moisture curing was found the be the most useful in case of Polyurethane based lightweight aggregate concrete [13]. The curing method i.e., moisture curing by jute bags, used complies with ASTM C511 [25] and ASTM C330 [26]

and the specimens were cured according to ASTM C192 [24]. The samples were taken out of jute bags an hour prior to testing.

(i) (ii) (iii)

Figure 7: (i) Casting of cylinders (ii) Casting of beams (iii) Moist Curing of samples

CHAPTER 4: EXPERIMENTATION

4.1 Basic Fresh/Hardened State Properties

4.1.1 Slump Test

The most prevalent test used to determine the flowability of fresh concrete is the slump test. It is performed by filling a mold with concrete and measuring the height of the formed mass. The results are then compared with ASTM C-143 [27]. It helps in optimizing the water to binder ratio and percentage of superplasticizer based on a specific flow level.

The freshly mixed concrete is poured in cone shaped steel mold and tamped with a steel rod to provide compaction. Then the cone is lifted and positioned upside down on the floor near the concrete. Meanwhile, the concrete will recede. Then the steel road was placed across the top of an upside-down cone to measure the slump. The distance between the top of slump and the rod is measured using scale as shown in Figure 8. The distance measured is the slump value of concrete. The level of slump is measured to the nearest 5mm.

Figure 8: Measurement of Slump Value

4.1.2 Fresh and Air-Dry Density

Fresh Density of the specimens was measured following ASTM C138 [28]. Firstly, the weight of the mold was measured using weight balance apparatus. After thorough mixing of the constituents in the pan mixer, the freshly mixed concrete was placed in molds in 3 layers each compacted with the help of a steel rod or mechanical vibrator.

The mold containing concrete was weighed. With the volume of mold known, use the following formula to calculate the fresh density of the concrete.

$$Fresh\ density = \frac{Mass\ of\ Specimen}{Volume\ of\ mold}$$

Air Density of the specimens was measured for 7, 14 and 28 days as per the procedure mentioned in ASTM 642 [29]. After 7 days of casting, the hardened concrete was weighed using weight balance apparatus in NICE Structures Lab and then using the following formula, air dry density was calculated. Same procedure was followed for 14- and 28-days air dry density of samples.

$$Air\ dry\ density = \frac{Mass\ of\ Specimen}{Volume\ of\ mold}$$

4.1.3 Absorption and Porosity

Following ASTM C 642 – 21 [29], the absorption of different samples of PU, Coated PU and Pumice based concrete was determined along with densities and percentage of voids in hardened concrete. Absorption and porosity help in determining the durability of specimen. The method includes oven drying the sample for a minimum of 24 hours at a temperature of 100 to 110°C. Allow it to cool down to room temperature and note down its oven dry mass (A). The process was repeated until any two successive results have a difference between them that is less than 0.5 percent of the lowest value determined. After drying, the specimen was submerged for at least 48 hours in water at about 21°. The procedure was repeated until an increase in mass of less than 0.5 percent of the bigger value can be seen between two successive measurements of mass of the surface-dried sample taken at 24 hours intervals. The surface of the specimen was dried using towel and its mass was determined (B) using mass balance.

The Absorption after Immersion was calculated using the following formula:

$$Absorption\ after\ Immersion = \frac{B-A}{A} \times 100$$

Now, by placing the sample in an appropriate container filled with tap water and letting it boil for five hours; the soaked, boiled, surface-dried mass was determined (C). It was allowed to cool down to room temperature for not less than 14 hours. Surface dry the specimen with the help of the towel and determine its mass. By using wire, the specimen was then suspended and the apparent mass in water was determined (D). To determine the Volume of pores, Bulk dry density (g1) and Apparent density (g2) were calculated using the following formulas:

$$Bulk\ dry\ density = \frac{A}{C-D} \times \rho$$

$$Apparent\ Density = \frac{A}{A-D} \times \rho$$

$$Volume\ of\ permeable\ pore\ space = \frac{g2-g1}{g2} \times 100$$

4.2 Mechanical Properties

The flexural and compressive strengths of concrete compositions were worked out according to the methods described in ASTM C293 [30] and ASTM C39 [31], respectively. The compressive strength at all ages is the mean value of the three 100 mm x 200 mm cylindrical specimens, while the flexural strength at all ages is the average of three 100 mm x 100 mm x 400 mm prismatic specimens. Samples were tested for mechanical strength at 7, 14 and 28 days.

4.2.1 Compressive Strength

At the ages of 7, 14 and 28 days, the samples casted were tested to determine the compressive strength as per the procedure mentioned in ASTM C39 [31]. After 7, 14 and 28-days curing, samples were placed inside the compression testing machine at Structures Laboratory of NICE, National University of Sciences and Technology (NUST). Before testing, caping was applied by using Plaster of Paris to provide uniform loading on the surface of the cylinder. Mean value of three cylinders was considered as the compressive strength of that mix. The test assembly is shown in the Figure 9 (a) and (b)**.** The compressive load was applied at rate of 0.25 MPa/second by compression testing machine.

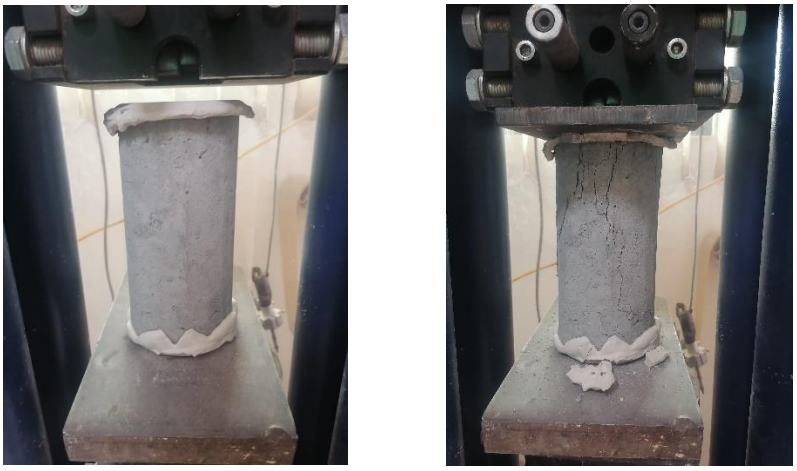

(a) (b)

Figure 9: (a) Test Setup for compressive strength (b) Cylinder failed in compression

4.2.2 Flexural Strength

12 beams, 4 for each matrix (A, B and C), having dimensions 100 mm x 100 mm x 400 mm, were casted for testing against flexure in accordance with ASTM C293/C293M [30]. The curing of beams was ensured till 28 days following the moisture curing method. As shown in Figure 10 (a), the beams were tested in center-point bending. A hydraulic press was used to apply pressure at a rate of 0.25 MPa/sec on a beam. The beam was simply supported by resting it on top of two roller supports. Load was applied until first crack developed at the bottom portion of the beam as it is evident in Figure 10 (b).

(a) (b)

Figure 10: (a) Test Setup for center-point bending test (b) Crack of beam initiated at bottom

4.2.3 Modulus of Elasticity

Elastic Modulus was determined as per the procedure mentioned in ASTM C 469 [32]. The cylinders were first fixed in the compressometer which is attached with a vertical dial gauge as shown in Figure 11. After fixing it in the compressometer, the whole assembly was placed in the compression testing machine. The load was applied up to 40 % of its strength and the strain values from the dial gauge were noted/recorded on video at 5 MPa increments of stress. The load is released and again applied till failure of the specimen and the values of stress and strain were noted in similar way. The stress corresponding to 40 percent of the ultimate load was noted down as S_2. The stress corresponding to a longitudinal strain, ε_1, of 50 millionths was determined. The longitudinal strain produced by stress S_2 was noted down as ε_2. Average of three cylinders was considered as Modulus of elasticity of that mix

formulation. Modulus of Elasticity was determined by following formula:

$$E = \frac{S_2 - S_1}{\varepsilon_2 - 0.000050} \ (psi)$$

Figure 11: Test Setup for Modulus of Elasticity

4.3 Durability Properties

4.3.1 Drying Shrinkage

Drying shrinkage is a measure of the change in length with age of a concrete specimen. The change in length may be due to external force caused by change in relative humidity, temperature, and moisture evaporation in the capillary pores of the specimen or due to heat of hydration as specimen ages. Drying shrinkage is an important parameter to be determined because capillary water loss leads to cracking leading to a remarkable decrease in the mechanical strength of the specimen.

6 prism specimens, 25 mm x 25 mm x 285 mm in dimension, were casted, 2 for each matrix (A, B and C). Moisture curing of these specimens were carried out for 3 days after which they were placed in the mold attached with a dial gauge. Drying Shrinkage test was conducted in compliance with ASTM C 596-18 [33]. Length comparator readings from the dial gauge were obtained at the ages of 4, 11, 18 and 25 days of air drying. Figure 12 shows the sample and the apparatus required to determine the drying shrinkage of concrete.

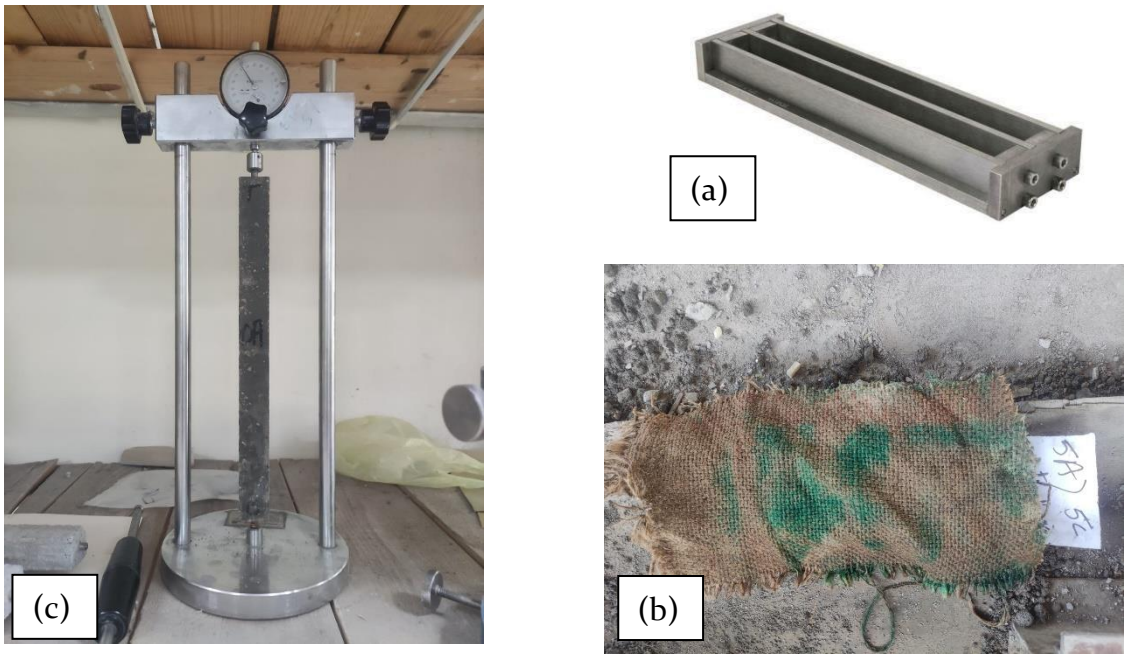

Figure 12: (a) Mold for Shrinkage Test (b) Curing of shrinkage test molds (c)Shrinkage mold setup in shrinkage apparatus

4.3.2 Electrical Resistivity

Electrical resistivity test of concrete is also known as Rapid Chloride Penetrability (RCP) test for concrete and is used to assess the durability of concrete [34]. It is a test that determines the chloride ion penetrability potential of concrete. Cylindrical specimens prepared are subjected to a standard voltage and the total electrical charge passing through the cylinder is measured. RCP provides an insight to the potential of a specimen to resist the chloride ion penetration, but it is unable to directly quantify chloride penetrability [34]. This test was conducted according to the specifications set by ASTM C1202 [35] and AASHTO T-227 [36].

Penetration of chloride ions into reinforced concrete (R.C.) structures is an important factor that must be considered in design and construction because it can lead to corrosion of the steel reinforcement and thus affect the durability of the overall structure [37]. Electrical Resistivity tells us about the porosity and microstructure of the concrete. Less or finer pores will result in greater electrical resistance which indicates greater durability. As a result, the ability of concrete to resist ion transfer when exposed to an electrical field can be used to describe the electrical resistivity of concrete [35].

For this research, the two-point uniaxial test method was chosen to determine the electrical resistivity of the cylindrical concrete samples, which involved placing a

concrete cylinder between two electrodes, which are generally parallel metal plates and using moist sponges in between the surface of specimen and the metal plate to ensure a proper electrical connection. The resistivity of specimens was measured using CMT Digital Resistivity Array Meter. The test set-up for uniaxial electrical resistivity test is shown in Figure 13.

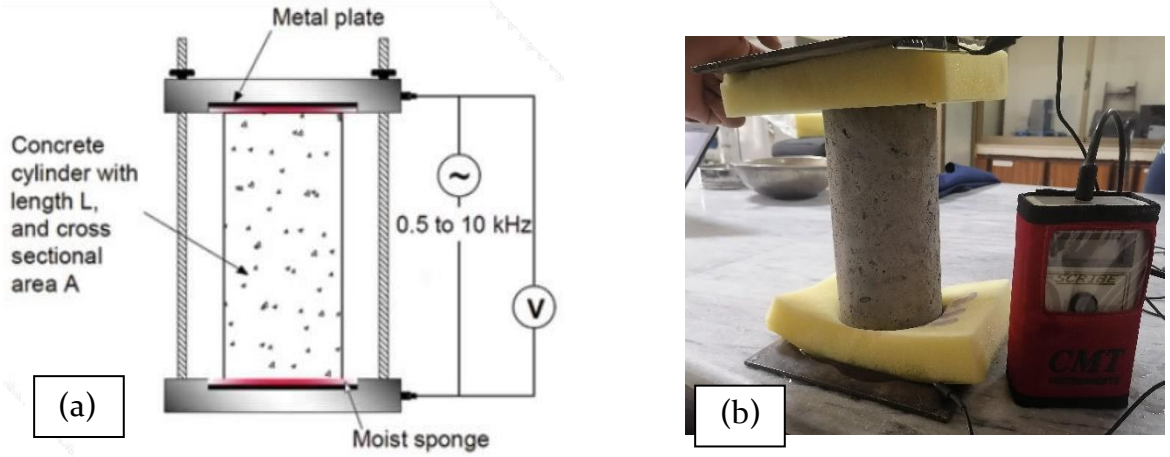

Figure 13: Test set-up for Uniaxial Electrical Resistivity Test

4.3.3 Freeze and Thaw Resistance

Freeze and thaw resistance helps in determining the Durability of concrete [38]. It helps to figure out the development of cracks integrated in a concrete specimen due to freezing and thawing. The qualities of lightweight aggregate and the freezing rate can affect freeze–thaw resistance, but the pore structure of the aggregate is the most important component. Lightweight aggregates with smaller pores and reduced pore volume can be resistant to freezing and thawing [39].

Adopting the standard CEN/TR 15177-06 [40], 5 cubes of 150 x 150 x 150 mm in dimensions were casted for each mix formulation i.e., for A, B and C, and placed them in tap water for 7 days. At the age of 21 days, each cube is sawed, perpendicular to the top surface, into a specimen that is 50 ±2 mm thick as shown in Figure 14.

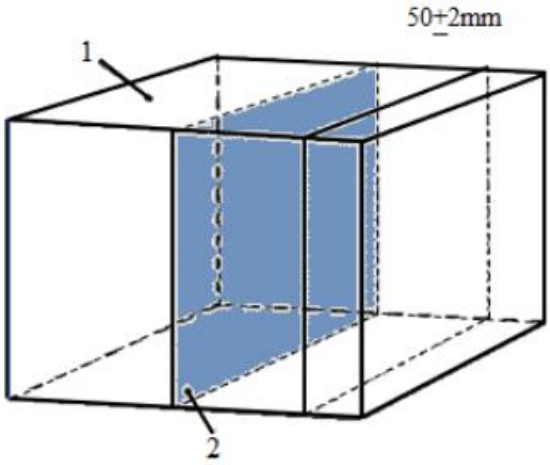

1 Top surface of specimen

2 Test Surface

Figure 14: Location of the test sample and test surface in sawn cube

After 25±1 days, rubber sheet was applied with glue to all the of the specimen's surfaces with the exception of the top surface as it had to be used for testing according to the standard adopted. In order to avoid loss of water, silicon was glued at the joints of concrete and rubber sheet. The edge of the rubber sheets ought to protrude 20mm from the surface. These were filled with deionized water up to 3mm depth. Saturation was carried out for 3 days prior to testing. These specimens were thermally insulated by wrapping Polystyrene foam around them as shown in Figure 15. Specimen were filled with deionized water up to 3mm depth and were stored in Climate Chamber present in Structures Lab, NUST Institute of Civil Engineering (NICE), NUST. They were covered with plastic sheet to avoid loss due to evaporation before storing them in Climate Chamber. The climate chamber was set according to the requirements of the standard i.e., the climate chamber was set for 21 cycles of 4 freezing hour limits and 2 thawing hour limits per cycle. The temperature of the cycles was maintained in the freeze-thaw chamber using programming as shown by the Table 12.

Table 12: Time and Temperature maintained during freeze-thaw cycle

Upper Limit		Lower Limit	
Time (hours)	**Temperature (°C)**	**Time (hours)**	**Temperature (°C)**
0	+24	0	+16
5	-3	3	-5
12	-15	12	-22
16	-18	16	-22
18	-1	20	-1
22	+24	24	+16

UPVT was carried out, as mentioned in CEN/TR 15177-06 [40] by using PUNDIT apparatus, on each specimen after 7, 14 and 21 days. Gel was applied on the contact surfaces of the transducers which were to be pressed on the marked contact surfaces of the specimen. The initial transit time (t_o) and transit time after n cycles (t_n) were determined which were used to calculate the internal structure damage i.e., relative dynamic modulus of elasticity (RDM) by using the following formula:

$$RDM = \left(\frac{to}{tn}\right)^2 x\ 100[\%]$$

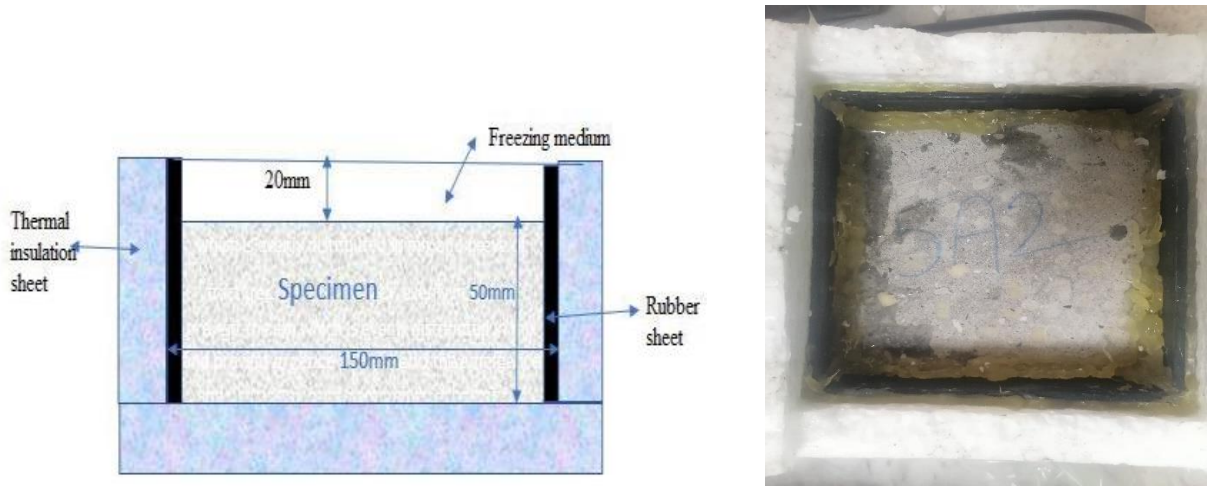

(a) (b)

Figure 15: (a) Test arrangement for Slab Test (b) Prepared Specimen

4.3.3.1 PUNDIT Test

Portable Ultrasonic Non-destructive Digital Indicating Tester is a versatile and convenient tool for checking the internal condition of concrete. It can detect cracks,

defects, and porosity. The tester employs a high frequency transducer that produces ultrasonic waves of between 30 KHz and 200 KHz. These waves are reflected by any defect in the material being tested. The reflecting transducer creates an audio tone which is then amplified and transmitted to the device where it is displayed as a waveform on the screen.

This test was conducted to work out the transit time i.e., pulse velocity of different specimens. Firstly, the device was calibrated, and gel was applied on the contact surfaces of the transducers which were to be pressed on the side surfaces of the sawed cubes. When pressed on the side surfaces of sawed concrete cubes, a waveform is generated on the screen of the PUNDIT device along with the value of the transit time in microseconds which was noted down.

4.4 Thermal Conductivity Test

Thermal Conductance is defined as the rate at which heat is transferred through a material. Thermal efficiency of a specimen is determined using the K-value or thermal conductance. Guarded Heat Flow Meter was used to determine the thermal resistance of a concrete disc specimen following the test procedure conforming to ASTM E 1530-99 [41]. The test and analysis of test results were conducted in U.S-Pakistan Center for Advanced Studies in Energy (USPCAS-E), NUST and the results of thermal conductance were reported.

Three concrete discs of 50 mm x 25 mm were casted for each mix formulation (A, B and C) and were sent to USPCAS-E for testing. The test setup involves positioning the specimen between a hotplate and a cold plate, as well as heat flux transducers (HFT). The testing temperature range was 0 to 50 degrees Celsius, which corresponds to the highest and minimum temperatures in Islamabad, Pakistan. Figure 16 (b) [41] depicts the testing assembly.

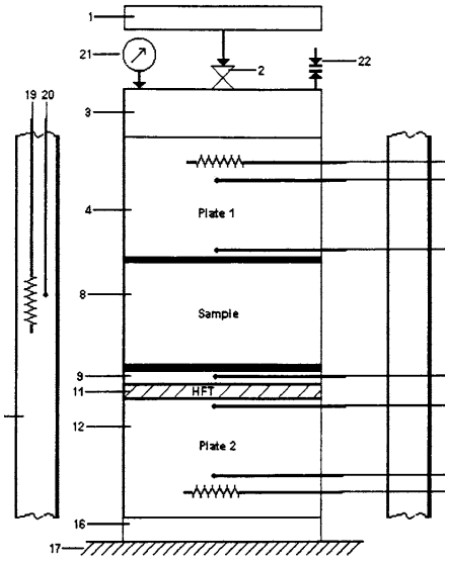

(a) (b)

Figure 16: (a) Discs casted for test (b) Test Assembly for Test

4.5 Scanning Electron Microscope (SEM)

Scanning electron microscope (SEM) analysis of concrete samples was conducted at School of Chemical and Material Engineering (SCME), NUST. SEM is a powerful and versatile analytical tool for the study of concrete. It is especially useful for the determination of chemical composition and microstructure of concrete, as well as for the study of pore size distribution. SEM also can be used to examine surfaces, such as those on concrete pavement, or surfaces that have been damaged by abrasion or corrosion.

A scanning electron microscope (SEM) is a very high-resolution electron microscope that produces an image by scanning a beam of electrons over a specimen surface while monitoring the intensity of the beam on an electronic detector. It works by placing an object under the action of an electron microscope's powerful beam of electrons. The beam passes through an attached lens that focuses it on the object being studied; this is called "scanning." The beam moves across the surface of the sample, generating thousands of points on its surface for imaging; this is called "electron micro graphing." Figure 17 (a) and (b) shows the SEM image of polyurethane and pumice-based concrete, respectively.

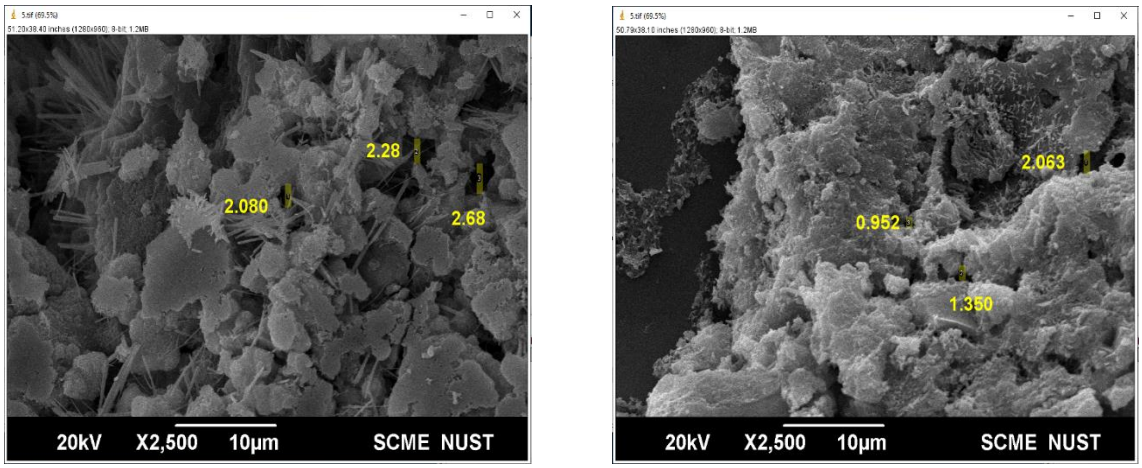

(a) (b)

Figure 17: (a) SEM of Polyurethane based concrete and (b) SEM of Pumice based concrete

CHAPTER 5: RESULTS AND DISCUSSION

5.1 Slump Test

Table 13 depicts the slump values for all 15 mix formulations. The results were between 55 and 80 mm. Replacing pumice aggregates (C-mix) with PU aggregates (A-mix) resulted in a slight reduction in the value of slump. It happened due to the high porosity of the PU aggregates, which absorb a lot of water and cement paste while lowering the workability of the concrete. Pre-coating of cement on PU aggregates slightly compensated this loss of workability. In fact, the slump values of B concrete were higher than those of A and C concretes. Improved workability was associated with lower water absorption of cement-coated PU aggregates. Hence, the water was involved in the liquefaction of fresh material. Superplasticizer addition did not significantly increase the workability. However, the suggested concrete proportioning made it possible to produce plastic concrete mixtures.

It is noted that the slump value is reduced by 21%, with the addition of 20% SF by weight of cement in PU-based LWC. SF particles have a larger surface area than cement particles; and hence, because the silica fume particles are finer than cement, some amount of superplasticizer have been adsorbed on their surfaces. Increasing the percentage of SF in the concrete, increases both the water and superplasticizer demand for the resulting mixture [42].

Table 13: Results of Slump Test

Serial	Formulation	Slump Values (mm)	Formulation	Slump Values (mm)	Formulation	Slump Values (mm)
1.	0A	70	0B	85	0C	80
2.	5A	60	5B	80	5C	75
3.	10A	60	10B	80	10C	75
4.	15A	60	15B	75	15C	70
5.	20A	55	20B	70	20C	65

5.2 Fresh and Air-Dried Densities

The average fresh densities for all 15 mix formulations are tabulated in Table 14. The fresh density and the air-dried density of the concretes at 28-days were significantly lower because of the low density of polyurethane aggregates. Mixes A and B showed fresh densities of 1870 kg/m^3 and 1757 kg/m^3, respectively with 10 percent silica fume. Their densities were 2.3–8.2% lower than that of the density of control pumice-based LWAC. The average air-dried densities for polyurethane, cement coated polyurethane and pumice based lightweight concretes are tabulated in Table 15, 16, and 17, respectively. After 28 days, the densities at 10% Silica Fume were 1829 kg/m^3 and 1666 kg/m^3 for mixes A and B, respectively. Therefore, the polyurethane-based concrete can said to be as a lightweight concrete [43]. With the addition of SF, the density values are reduced. As the SF particles have less density than that of cement particles, hence the cement replacement by silica fume lowered the overall density of the concrete. The fresh density of LWC was significantly affected by the cement coating of polyurethane aggregates: the average difference between the densities of mixes A and B was 107.2 kg/m^3 . When the PU foam aggregates are precoated with the cement, the density of the cement coated PU particles increases that caused an increase in the amount of the foam in the concrete mix hence, decreasing the overall density of cement coated polyurethane-based concrete.

Table 14: Average Fresh Densities

Serial	Formulation	Avg Fresh Density (kg/m^3)	Formulation	Avg Fresh Density (kg/m^3)	Formulation	Avg Fresh Density (kg/m^3)
1.	0A	1897	0B	1865	0C	1932
2.	5A	1893	5B	1787	5C	1931
3.	10A	1870	10B	1757	10C	1914
4.	15A	1869	15B	1712	15C	1859
5.	20A	1805	20B	1677	20C	1828

Table 15: Average Air-dried Densities of PU-based LWC (A mix)

Serial	Formulation	Average Air-dried densities (kg/m^3)		
		7 days	**14 days**	**28 days**
1.	0A	1856	1855	1840
2.	5A	1855	1853	1830
3.	10A	1854	1838	1829
4.	15A	1821	1815	1812
5.	20A	1780	1777	1750

Table 16: Average Air-dried Densities of Cement Coated PU-based LWC (B mix)

Serial	Formulation	Average Air-dried densities (kg/m^3)		
		7 days	**14 days**	**28 days**
1.	0B	1824	1800	1755
2.	5B	1773	1721	1688
3.	10B	1753	1716	1666
4.	15B	1695	1662	1614
5.	20B	1641	1620	1570

Table 17: Average Air-dried Densities of Pumice based LWC (C mix)

Serial	Formulation	Average Air-dried densities (kg/m^3)		
		7 days	**14 days**	**28 days**
1.	0C	1884	1800	1755
2.	5C	1880	1721	1688
3.	10C	1753	1716	1666
4.	15C	1712	1662	1614
5.	20C	1677	1620	1570

5.3 Mechanical Strength

The compressive strength of concretes at the age of 7, 14 and 28 days are shown in figures 18, 19 and 20, respectively. The flexural strength at 28 days is shown in Figure 21.

Incorporating PU-foam aggregates significantly reduced the mechanical strength of concrete. Many studies have already shown that the mechanical characteristics of concrete have been significantly reduced because of the utilization of Lightweight

Aggregates (LWA) [44–47]. This reduction can be explained by the high porosity and the poor mechanical characteristics of LWA. It should be observed that the rupture mechanism of the lightweight aggregate samples is differs from the rupture mechanism of the Normal Weight Concrete (NWC), as proved in the literature. In the case of lightweight aggregate concrete, rupture occurred not only at the mortar matrix and lightweight aggregate interface, but also at the center of the lightweight aggregate, which serves as the weak link in the lightweight aggregate concrete microstructures. ITZ in the normal weight concrete has poor properties compare to the other concrete parts, so the failure occurred mainly in ITZ [44-47].

The discussion above shows that the strength of LWA is a constraint for concrete; the transition zone is not the weakest link in the LWAC. Once the strength of mortar reaches a particular level, the corresponding strength of LWAC will no longer increase.

5.3.1 Effect of age on the development of Strength

The development of strength of PU, cement coated PU and Pumice based LWC is depicted in Figures 18, 19 and 20. For various mixes, the uncoated polyurethane based LWC has a faster hardening factor than pumice-based LWC in the initial setting phase, achieving 62 % of the 28-day strength within 7 days with 10% silica fume replacement.

Incorporating a mineral admixture into concrete affects the cement hydration rate and the development of strength. It is evident that the development of pozzolanic reaction, in which a continuous process of pore miniaturization and structural improvement occurs in the transition zone, may be related to both the rate of strength development and the ultimate strength of concrete made with mineral admixtures [48].

5.3.2 Impact on compressive strength by cement replacement with SF

Results indicate that the 10% SF provided maximum compressive strength at all ages. The densified effect of silica fume which decreases the porosity at an early age, accounts for the increase in compressive strength brought on by the addition of silica fume, but at a later age, a pozzolanic reaction takes place, in addition to the densified effect of silica fume, in which calcium hydroxide released from cement hydration reacts with the silica fume to produce a filling effect in the empty spaces between the cement and other powder particles [13]. The decrease in compressive strength after 10% Silica Fume may be attributed to these mentioned factors: the effective water to cement ratio rises with an increase in percentage of silica fume and the pozzolanic reaction is also a delayed effect. It takes more time for complete reaction to take place to achieve a higher strength

than the regulated specimen; hence, adding silica fume brings a change in strength by two principles: impact on cement hydration by the dilution effect and the chemical influence. The dilution effect is a result of the cement replacement by silica fume, which equates to an increase in water to cement ratio [49, 50]. On the other hand, the chemical effect represents an increase in strength due to the reaction of the mineral admixture with calcium hydroxide, producing a fibrous CSH. After replacing the cement with Silica Fume by 10%, the dilution effect dominates the chemical effect. Therefore, a decrease in compressive strength is observed up-to 28 days of age. After the age of 28-days, a pozzolanic reaction takes place between the mineral admixture and Calcium Hydroxide (CH), which is not investigated in the scope of this study [50].

As shown in Figure 21, LWAC (Lightweight Aggregate Concrete) with SF exhibits marginally greater flexural strength at 28 days compared to the comparable mix without SF, with an average increase of 1.42%. The comparable flexural strength values for mixes A, B, and C proved that the LWA is the weakest link in LWAC, not the interfacial transition zone between the aggregate and the matrix. Therefore, a further significant increase in flexural strength cannot be achieved by the addition of SF.

5.3.3 Effect of preliminary cement coating on PU aggregate

Pre-cement coating of the PU foam particles results in a 33% reduction in the compressive strength between A and B mix formulations. This finding appears to support the earlier hypothesis that pre coating of PU aggregates with cement increases the density of PU aggregate that leads to increase the PU aggregate proportion in the concrete mixture. It also led to a reduction in the amount of cement that had to take part in the hydration reaction and thus lowering the overall mechanical characteristics of the concrete. In this case, cement paste on the PU particles only serves to increase the porosity and adversely affects the mechanical strength. The mechanical properties of the B mix were too low in relation to its density to be categorized as moderate-strength lightweight aggregate concrete. In contrast, A and C mix at 10% silica fume replacement, met the criteria for structural LWAC as established by ACI 213 [51] and ASTM C 330 [26]. In fact, the ACI 213 demands that the Structural Lightweight Aggregate Concrete (SLWAC) (i) have a minimum cylindrical compressive strength of 17 MPa at 28 days, (ii) have a corresponding air-dry density of 1850 kg/m^3 or less, and (iii) be entirely made of lightweight aggregate or a combination of lightweight and normal weight aggregates [51]. As per the specifications of ASTM C 330, the coarse aggregate bulk density of the

lightweight aggregate utilized in the structural lightweight aggregate concrete must be less than 880 kg/m^3, that is the case for PU aggregates [26].

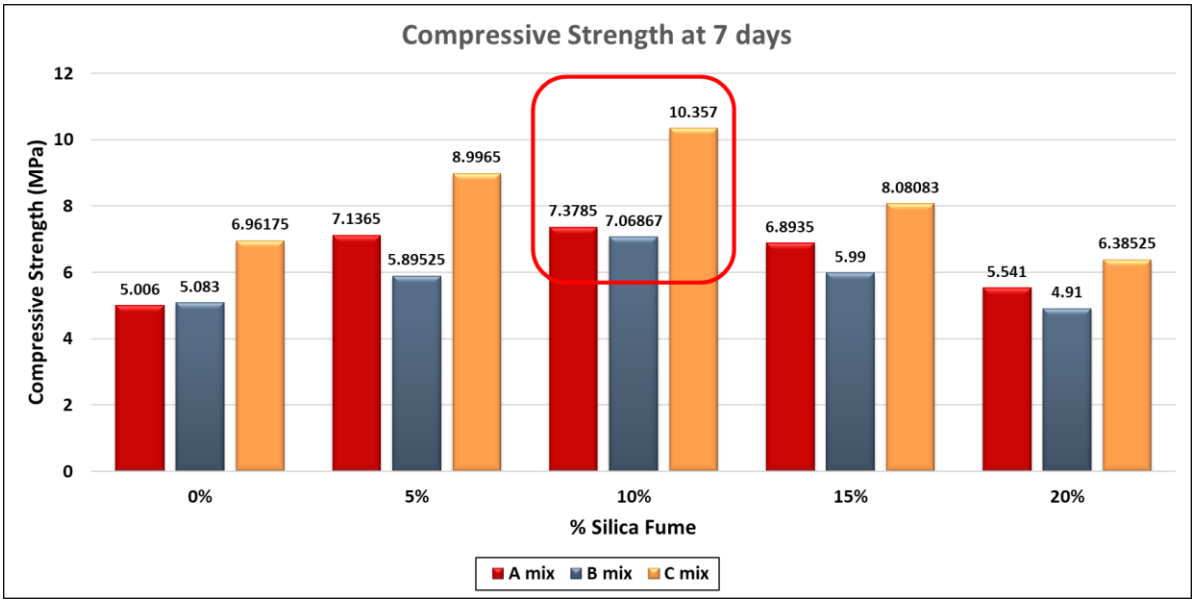

Figure 18: 7-days Compressive Strength Test Results for Pumice based LWAC (C mix), PU based LWAC (A mix) and Cement Coated PU LWAC (B mix)

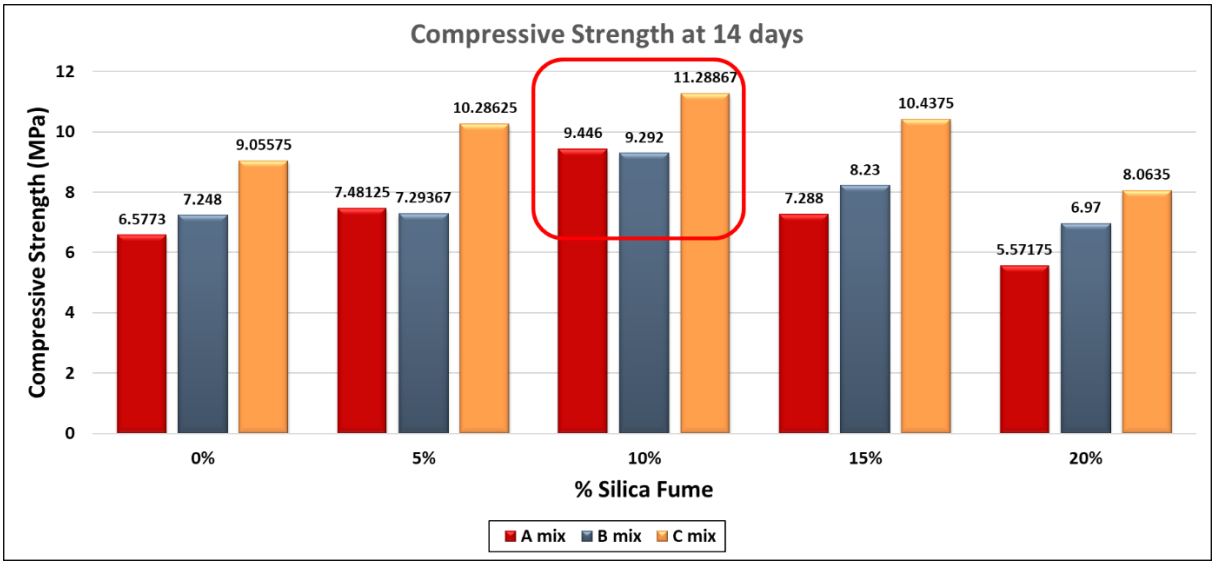

Figure 19: 14-days Compressive Strength Test Results for Pumice based LWAC (C mix), PU based LWAC (A mix) and Cement Coated PU LWAC (B mix)

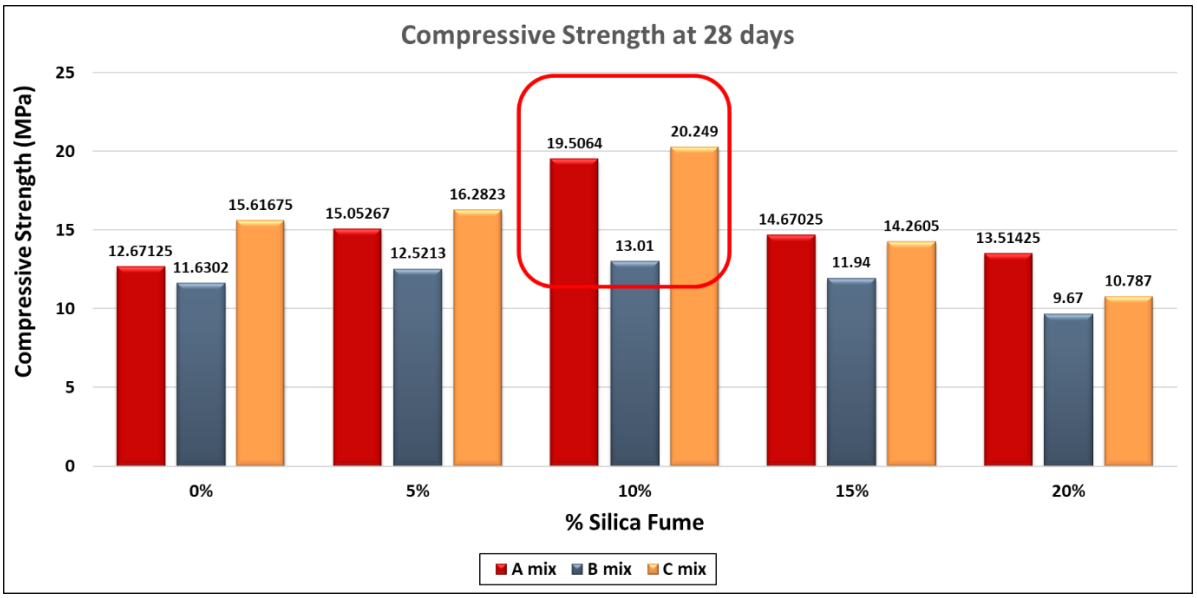

Figure 20: 28-days Compressive Strength Test Results for Pumice based LWAC (C mix), PU based LWAC (A mix) and Cement Coated PU LWAC (B mix)

The results of the flexure strength test indicate that the B mix has the least flexural strength out of the three mixes, whereas the results with and without silica fume are much more comparable.

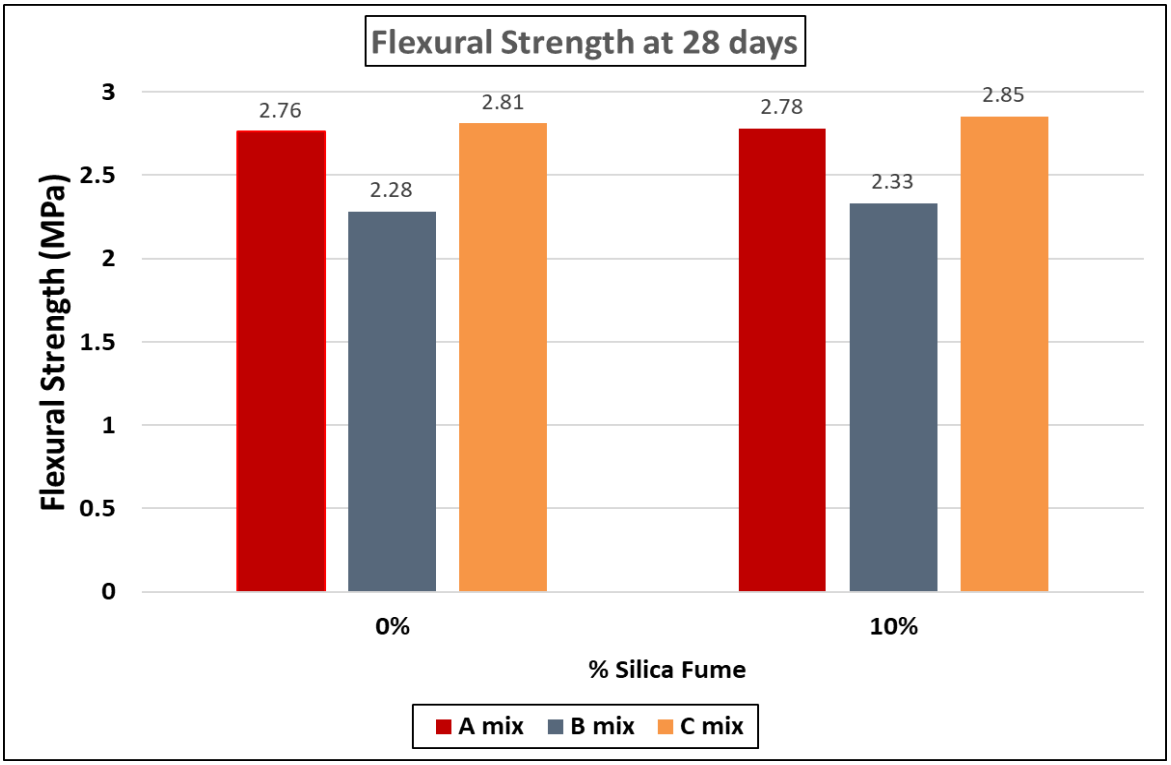

Figure 21: 28-days Flexural Strength Test Results for Pumice based LWAC (C mix), PU based LWAC (A mix) and Cement Coated PU LWAC (B mix)

5.4 Modulus of elasticity

At each load level, longitudinal strains for cylinders under compression were noted. Stress-Strain curves were formed up to a load level of 40 percent of compressive strength. The elastic modulus (E) is altered by the presence of lightweight aggregate, albeit the impact of lightweight aggregate on Elastic modulus values is often less significant [52, 53, 54]. For instance, Aamr-Daya et al. [53] found that compressive strength and young's modulus of a lightweight cement composite are both reduced by 67–77% and 49%, respectively, when flax by-products at 10 percent are added as compared to a composite without flax particles. Pumice based LWAC shows the greater values of the elastic modulus as compared to PU based LWAC. As the mechanical strength is increasing with the age of concrete, the elastic modulus is also increasing due to increased stiffness.

5.4.1 Effect of preliminary cement coating on PU aggregate

Due to the porous nature, Polyurethane foam has a low modulus of elasticity; hence it was hypothesized that increasing the LWA content due to their preliminary coating would lower the E-values of LWAC. When compared to the E-value of uncoated PUR-based LWAC, this drop was 38% at 10% silica fume.

5.4.2 Impact on elastic modulus by cement replacement with silica fume

A comparison of the modulus of elasticity across mixes A, B and C utilizing 0-20% of cement replacement by silica fume is shown in Figures 22, 23, and 24. When compared to the concrete without SF, PU concrete with 10 percent SF has higher E values. It should be noted that the volume of the paste in mixes with silica fume as cement replacement is comparably higher than the volume of paste in a corresponding mix without silica fume. This behavior could be explained by the use of silica fume as a partial substitution of cement in the mixes, which densifies the concrete and reduces strain under compression at the transition zone. As a result, the static elastic modulus of the LWA concrete is improved to some extent.

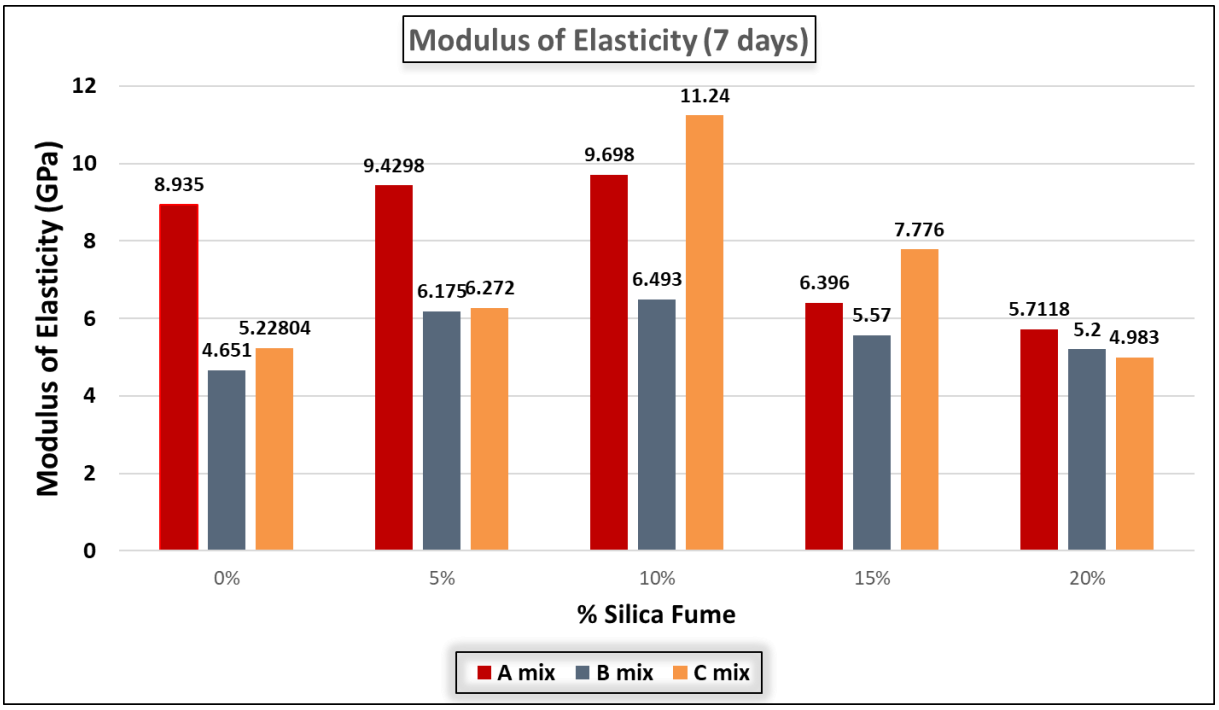

Figure 22: 7-days Modulus of Elasticity Test Results for Pumice based LWAC (C mix), PU based LWAC (A mix) and Cement Coated PU LWAC (B mix)

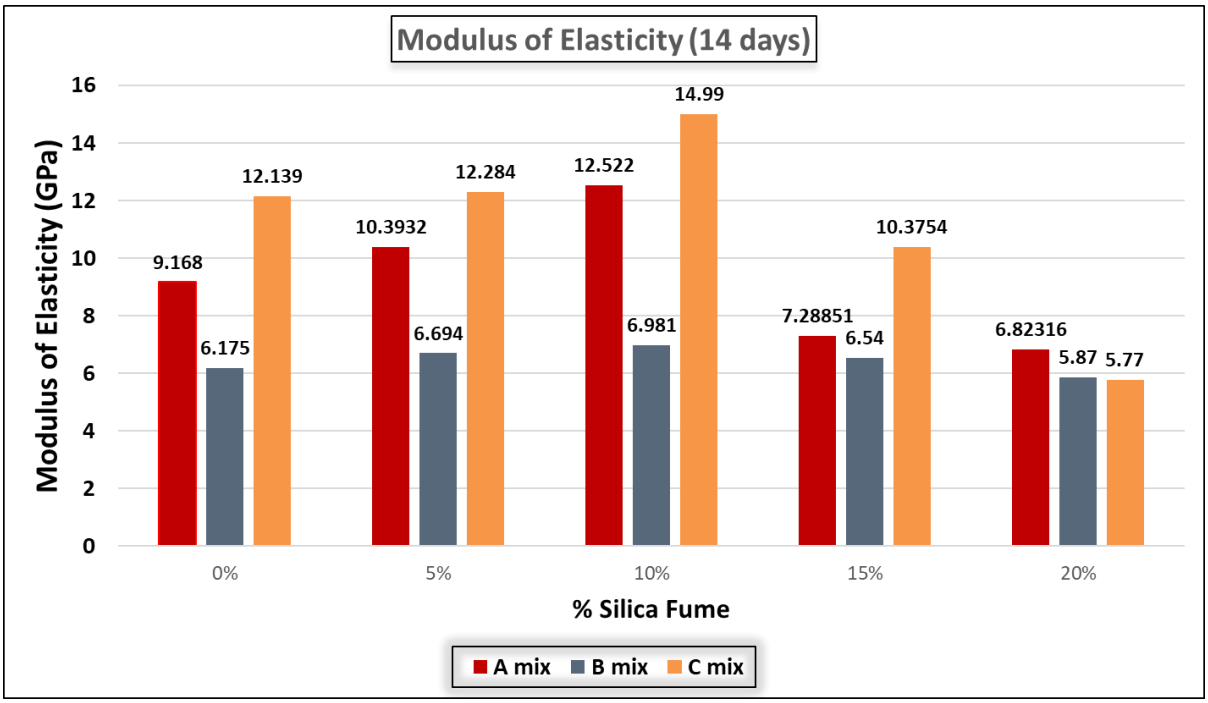

Figure 23: 14-days Modulus of Elasticity Test Results for Pumice based LWAC (C mix), PU based LWAC (A mix) and Cement Coated PU LWAC (B mix)

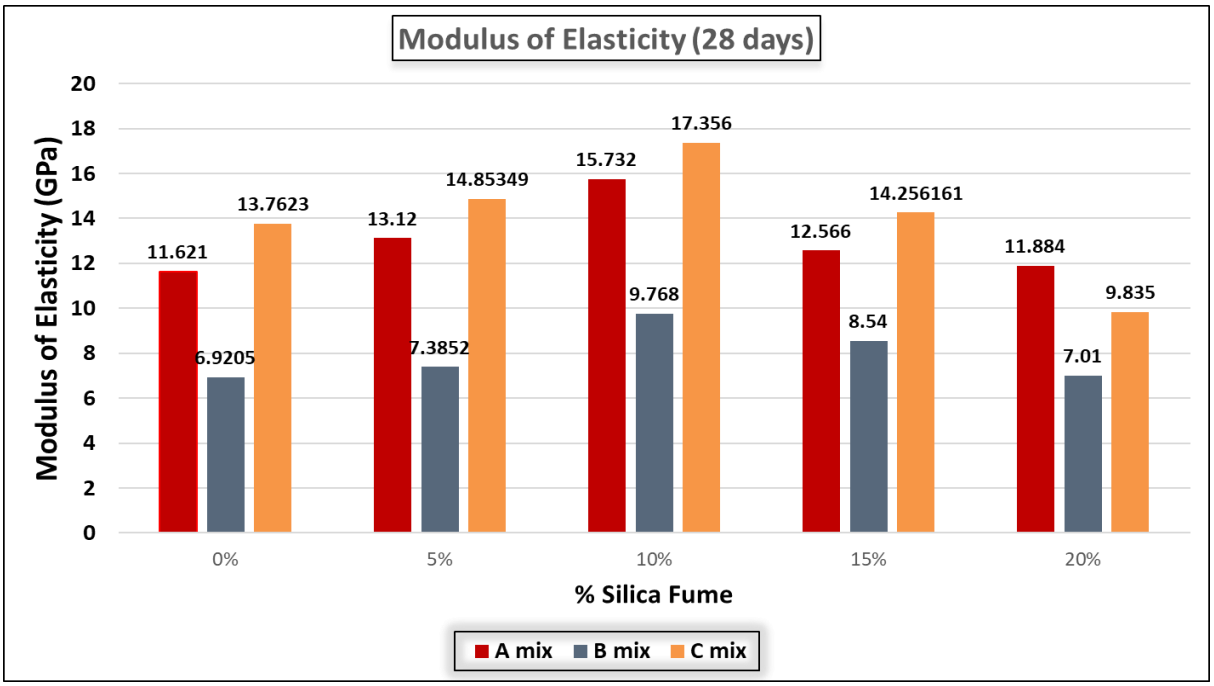

Figure 24: 28-days Modulus of Elasticity Test Results for Pumice based LWAC (C mix), PU based LWAC (A mix) and Cement Coated PU LWAC (B mix)

5.5 Permeable Voids and Absorption of hardened concrete

Water was added in concrete as mixing water that relates to water/binder ratio. Lightweight concrete's higher absorption and permeable voids (Table 18 and 19) enhance and expedite water diffusion and consequently material mass loss. The most porous concrete (A mixes) had the highest 28-day absorption and volume of permeable voids due to the uncoated PUR foam content (Table 18 and 19). These findings are comparable to those of Saradhi Babu et al. [55], who found that concretes with large proportion of LWA exhibited higher moisture migration in water absorption test. They attributed part of the phenomenon to possible microcracking produced by low-density aggregate shrinkage. Tables 18 and 19 show a direct correlation between absorption percentages and the volume of permeable voids in concretes. When pumice aggregates (C mix) were replaced with PUR-foam aggregates (A mix), for the constant water content, the volume of permeable voids and absorption percentage was increased, which was linked to the increase in porosity.

Water flow across a porous media comprised of both water flow through the cementitious matrix and flow through LWA. Mass transfers in this flow are influenced by number of factors pattern in addition to pore volume. The pore diameter as well as the structure and connectivity of the porous network, play a role in mass flow across

the medium [56]. By this perspective, it was able to lower both the permeability and the density of the concrete by altering cementitious phase composition and increasing LWA content.

5.5.1 Effect of preliminary cement coating on PU aggregate

The permeable voids volume and absorption were lower in the concrete made with cement coated PU aggregate than in concrete made with uncoated PU aggregate. This is due to the fact that cement coated PU foam aggregates had lesser absorption percentage than uncoated PU foam aggregates.

5.5.2 Effect of cement replacement by silica fume

Silica fume densifies the concrete pore structure due to its finer particle size. As a result, as the percentage of SF used to replace the cement increases, the permeability and absorption of hardened concrete decreases.

Table 18: Average Absorption percentage in hardened concrete

Serial	Formulation	Absorption (%)	Formulation	Absorption (%)	Formulation	Absorption (%)
1.	0A	6.1	0B	4.8	0C	5.8
2.	5A	5.1	5B	3.5	5C	4.3
3.	10A	4.4	10B	3.4	10C	3.9
4.	15A	3.1	15B	2.9	15C	3.1
5.	20A	2.8	20B	2.5	20C	2.5

Table 19: Volume of permeable voids in hardened concrete

Serial	Formulation	Permeable voids (%)	Formulation	Permeable voids (%)	Formulation	Permeable voids (%)
1.	0A	10.9	0B	9.7	0C	10.8
2.	5A	8.1	5B	6.8	5C	7.6
3.	10A	7.7	10B	6.5	10C	7.4
4.	15A	5.9	15B	5.5	15C	5.5
5.	20A	5.4	20B	4.9	20C	5.2

5.6 Drying Shrinkage

The capillary tensile force produced because of water loss from the concrete causes drying shrinkage. Drying shrinkage predominates over autogenous shrinkage in the water to binder ratio range studied in this work [57–59].

The drying shrinkage test was conducted as per the procedure mentioned in ASTM C 596-18 [33], with readings taken at for 4, 11, 18 and 25 days. The shrinkage test results shows that the drying shrinkage for all three specimen is less than 350 micrometers, which is significantly below the 600 micrometers limit set by ASTM C 157 [60] and AS 3972-2010 [61]. Furthermore, the test findings shows that PU-based concrete (A mix) has the largest length change owing to drying shrinkage, followed by Coated PU-based concrete (B mix), and finally a control mix of pumice-based concrete.

According to Neville [43], using lightweight aggregate produced greater shrinkage, because of the lower lightweight aggregate modulus of elasticity [62]; also, aggregates having strong absorption characteristics are linked to significant shrinkage in concrete [63]. Because of the high absorption characteristics, there is a greater demand for water and a higher w/c ratio, resulting in larger drying shrinkage deformations [64]. The heat of hydration released throughout the hydration process of each formulation can explain these test results.

5.6.1 Effect of preliminary cement coating on PU aggregate

Figures 25 and 26 shows the drying shrinkage of moist cured LWC with and without silica fume but having the same water content after 4, 11, 18 and 25 days. The drying shrinkage of PU-based concrete mix is reduced when they are pre-coated with cement, as seen in the figures. For 4, 11, 18 and 25 days curing without silica fume, the drying shrinkage values for mix B (Coated PU) are 56, 173, 271 and 301 micrometers respectively; and for 4, 11, 18 and 25 days curing with 10% SF, the drying shrinkage values were 52, 167, 270 and 298 micrometers respectively. The shrinkage of hydrated cement paste for NWC is directly related to the W/C ratio which ranges from around 0.2 to 0.6 [65]. When W/C ratio is higher, excess water is lost from capillary pores as it dries, causing more shrinkage. A lower W/C ratio in NWC results in less drying shrinkage [66].

5.6.2 Impact on drying shrinkage by cement replacement with silica fume

At 4, 11, 18 and 25 days of moisture curing, the drying shrinkage of concretes without SF and containing 10 percent of SF is shown in Figures 25 and 26, respectively. The drying shrinkage values for mix A (PU) after 25 days are 337 and 345 micrometers with and without silica fume, respectively. The strains for mix B (Coated PU) are 298 and 301 micrometers, whereas the strains for mix C (Pumice) are 188 and 197 micrometers with and without silica fume, respectively. For all of the mixes, there is a tendency of increased drying shrinkage as the duration of moisture curing increases. At 4, 11, 18 and 25 days of moist curing, the drying shrinkage of SF concrete is equivalent to that of the control mixes.

This agrees well with the findings of Carette and Malhotra (1983a) [67]. The permeability and pore size of concrete are lowered by SF, which retards the rate of drying shrinkage. Besides, it densifies the concrete microstructure and lowers the size of capillary pores, raising capillary pressure resulting in more and faster drying shrinkage rate [68]. Both phenomena can be used to explain how silica fume affects drying shrinkage. The increased water content due to PU foam particles can help to balance the two opposing effects of SF in drying shrinkage of PUR-foam concrete.

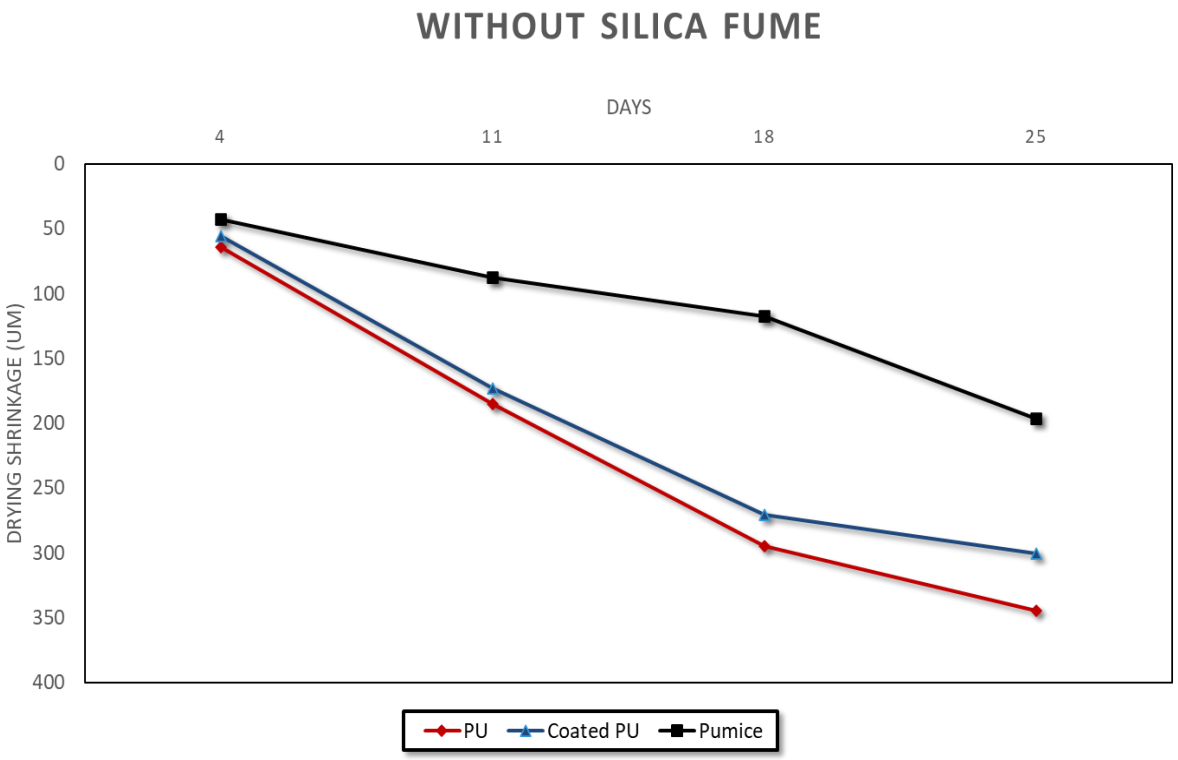

Figure 25: Shrinkage Test Results without silica fume

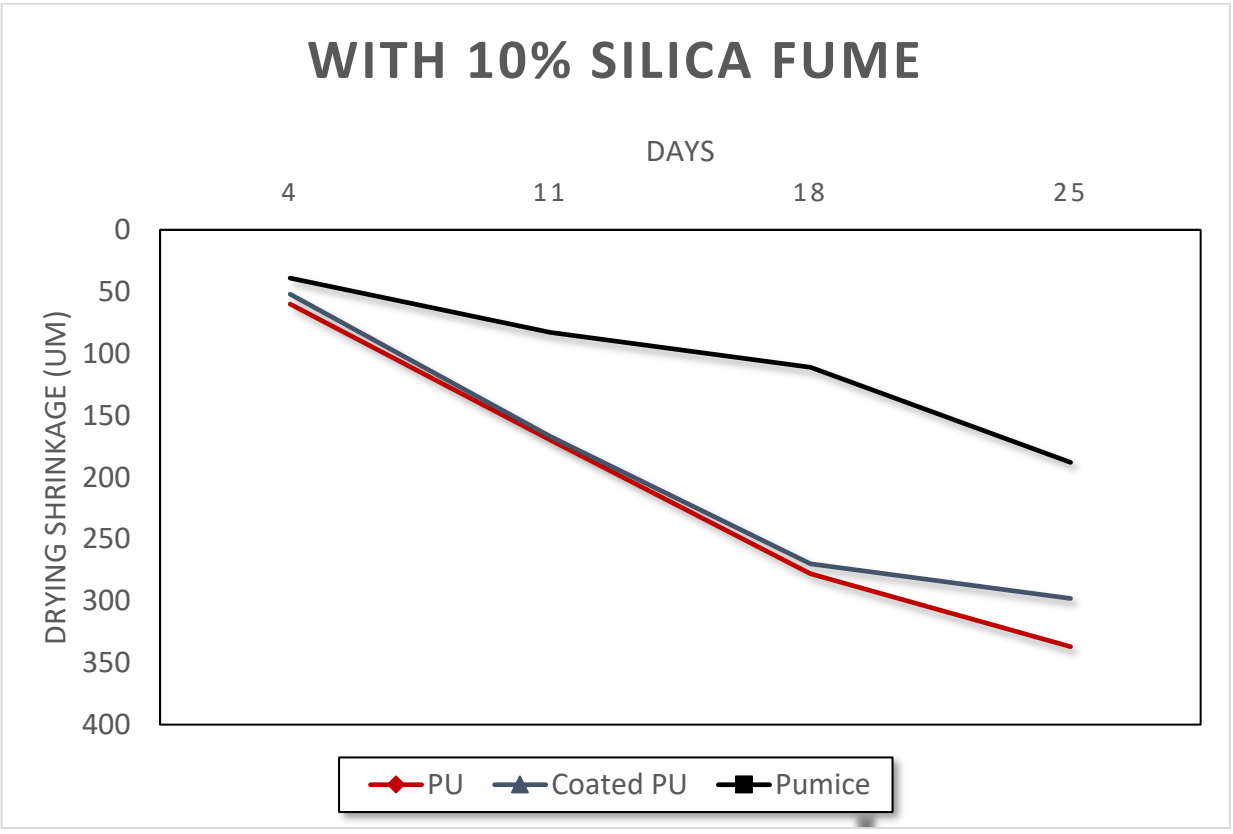

Figure 26: Shrinkage Test Results with silica fume

5.7 Electrical Resistivity

The Rapid Chloride Penetrability (RCP) Test, which is based on the ASTM C1202 [35] and AASHTO TP95-11 [36] standards, was utilized to determine the electrical resistivity. This test was performed after the concrete had been allowed to cure in wet conditions for 28 days and then dried in the air for one day. Table 21, based on ASTM C1202 [35] and AASHTO TP95-11 [36], specifies the various limits for Chloride Ion Penetrability based on electrical resistivity data. Table 20 summarizes the data obtained of the dry specimen**.** According to Table 21, all of the samples had electrical resistivity greater than 14 kΩ.cm at 10% silica fume incorporation, which lies in the 'moderate' chloride ion penetrability range**.** This means that when exposed to situations where chloride particles may pose a threat to the steel wire-mesh reinforcement embedded into the mortar layers, mortar layers for all mix formulations with more than 10% silica fume content will provide moderate resistance.

The utilization of lightweight aggregate in the concrete does not always imply increased chloride ion penetration [69]. For LWC and NWC with equivalent water to cement ratios, Sugiyama et al. [70] and Chia and Zhang [56] showed similar rates of chloride ion penetration. They claim that the application of denser outer layer of lightweight aggregate and a stronger interfacial zone of mortar with the lightweight aggregate can help to minimize the chloride ion penetration into lightweight aggregates. In LWAC, the characteristics of the cementitious matrix have a significant impact on mass transfers [69,70]. The ionic diffusion within LWAC was mostly influenced by the composition of mortar matrix and properties of ITZ [69]. There is an optimum cement content that allows to reduce chloride diffusion.

Table 20: Electrical Resistivity Test Results for Pumice based LWAC (C mix), PU based LWAC (A mix) and Cement Coated PU LWAC (B mix)

Electrical Resistivity (kΩ·cm)					
% Silica fume	**0**	**5**	**10**	**15**	**20**
A mix	7.4	9.975	14.275	16.075	17.985
B mix	10.05	14.06	18.175	23.12	23.33
C mix	9.84	11.84	16.95	18.475	19.225

Table 21: Comparison of chloride penetrability levels established for standards based on electrical resistivity (AASHTO TP 95 [36]) and charge passed (ASTM C1202 [35])

Sr. No.	**Penetration of Chloride Ion**	**AASTHO TP 95 -11 [36] (kΩ·cm)**	**ASTM C1202 [35] (Coulombs)**
1.	High	<12	>4000
2.	Moderate	12 to 21	2000 to 4000
3.	Low	21 to 37	1000 to 2000
4.	Very Low	37 to 254	100 to 1000
5.	Negligible	>254	<100

5.7.1 Effect of preliminary cement coating of PU aggregate

The test results also show that cement-coated PU aggregate concrete mix had the highest resistivity to chloride ions, followed by control mix i.e., Pumice-based concrete mix and finally uncoated PU-based LWAC sample. The low electrical resistivity for the uncoated PU aggregate mix sample may be due to the increased porosity as a result of adding PU foam in sample. This result, which is already mentioned in absorption and permeability test, suggests that the cementitious matrix has a decreased porosity.

5.7.2 Impact of cement replacement with silica fume

Dilution effect outweighs the chemical effect, while replacing cement by silica fume. At 28-days, the reduction in porosity due to finer particle size of silica fume manifested itself, resulting in silica fume samples having a denser pore structure and higher electrical resistance than control samples.

5.8 Thermal Conductivity

The DTC 300 Thermal Conductivity Meter (Guarded Heat Flow Meter) in USPCAS-E, NUST, was used to determine the thermal conductivity (K-value). Table 22 depicts the values of the thermal resistance (R-value) and thermal conductance (K-Value) tests performed on circular discs of 50 mm x 20 mm**.** The average thermal conductance values at three different temperatures in the temperature ranges of 0-50◦C, which is a representative of the maximum and minimum temperatures in Pakistan, are tabulated.

The average thermal conductance values of the three samples are within ± 1% of one another. The reason for this minute discrepancy is because the PU foam and Pumice aggregates are principally responsible for the insulation properties. The average thermal conductivity of a concrete sample is typically 1.5– 2.7 W/(m.K.) [71] and that of EPS insulation is 0.0313 W/(m.K.) [72]; hence, as the thicknesses of the concrete discs are almost equal, the resulting thermal conductivity of the three samples will be nearly identical.

Table 22: Thermal Conductivity Test Results

Formulation	Thermal Resistance R-Value (m^2K/W)	Thermal Conductivity K-value (W/mK)
Pumice Based LWC	0.0456	0.526
PU based LWC	0.062	0.371

The thermal conductivity values of PU-based LWC can also be compared to those of conventional residential building materials in Pakistan, as shown in Table 5.8.2. Autodesk® Green Building Studio was used to extract the values of conventional construction components. The thermal efficiency offered by adding PU foam aggregate

is confirmed by the K-value for PU-based LWC, which is almost 3-3.5 times less than that of precast concrete and conventional concrete masonry units and 1.5 times less than that of traditional brick masonry in residential homes.

Table 23: Thermal Conductivity Values for a typical building in Pakistan

Building Component	**K-Value (W/m2K)**
Concrete Masonry Units	1.299
Precast Concrete	1.045
Brick Masonry	0.539

5.9 Freeze and Thaw Resistance

To assess the internal structure damage caused by freeze-thaw on the LWACs, the slab test procedure CEN/TR 15177 [40] was used. An ultrasonic pulse transit time test was used to determine the degree of internal structural damage. After determining transit time, the RDM was determined and findings are tabulated in the Table 24.

Table 24: Relative Dynamic Modulus of elasticity

Formulation	**Relative Dynamic Modulus of Elasticity (RDM)**		
	Number of Freeze-Thaw cycles		
	7	**14**	**21**
10A	0.98391 ± 0.12	0.96917 ± 0.03	0.95199 ± 0.09
10C	0.96908 ± 0.02	0.91430 ± 0.07	0.88701 ± 0.11

The addition of PUR-foam aggregate reduced internal structure damage. This might be because PU foam is very porous and has a high permeability, which allows water to escape during freezing without causing aggregate damage i.e., it provides adequate room for freezing water without damaging the samples. Small deterioration is brought on by the freeze-thaw action in denser microstructure, and the PU foam aggregate forces cracks to stop or alter their trajectory. With the addition of PU aggregate foam and Silica

fume, air content is enhanced. Greater air content in the formulation results in less internal structure damage. Demirboga et al., ascribed the improvement in freeze and thaw resistance of SF mortars to the decrease in level of saturation in the specimens brought on by self-desiccation [73]. According to Zhou et al., Silica Fume makes non-air entrained mortar more resistant to freezing and thawing [74].

5.10 Scanning Electron Microscope (SEM) observations

The microstructure of the interfaces of mortar with polyurethane foam and mortar with Pumice aggregate, of newly broken LWAC cylinders are depicted in Figure 27 and 28, respectively. The samples were taken from pieces of cylindrical specimens that were analyzed in compression and inspected without any special preliminary treatment (drying or polishing). The interfacial transition zone (ITZ) has substantial influence on the mechanical behavior and transfer characteristics of cement-based composites. "Wall effect" that occurs on the normal weight aggregates surface and micro-bleeding i.e., the local water buildup under the aggregates in vibrated concrete, are the two main processes that are often responsible for the poor qualities of this zone. A Water to Cement ratio gradient produced by the first phenomenon near coarse aggregates, while the second phenomenon can cause this W/C ratio gradient to be rather heterogeneous [75]. The porosity and type of aggregates as well as the bleeding and porosity of the cement paste surrounding the aggregates all affect the properties of ITZ. These factors cause ITZ in LWC to deviate significantly from that of NWC [76]. On expanded clay aggregate concrete, Zhang and Gjørv [77] demonstrated how the porous surface of light weight aggregate enhanced the interfacial connection between aggregate and cement paste. Interconnecting sites that the rough surface of the lightweight aggregates produced, which led to a thick and homogenous ITZ with the mortar, were used to explain this phenomenon. Additionally, Lo and Cui [78] showed that the "wall effect" which manifests in NWC, does not exist on the Interfacial Transition Zone of Lightweight Aggregate Concrete. They determined that the ITZ that resulted was substantially less than for normal aggregate, measuring just approximately 5– 10 m broad. The cement paste penetrated the surface porosity of PU aggregate, which is big enough for the development of cementitious microstructure, as shown in Fig. 27, demonstrating strong bond between the cementitious matrix and the Polyurethane foam particles. No "wall effect" was

noticed at the interface between Polyurethane foam aggregate and cement mortar, for the observation scale considered.

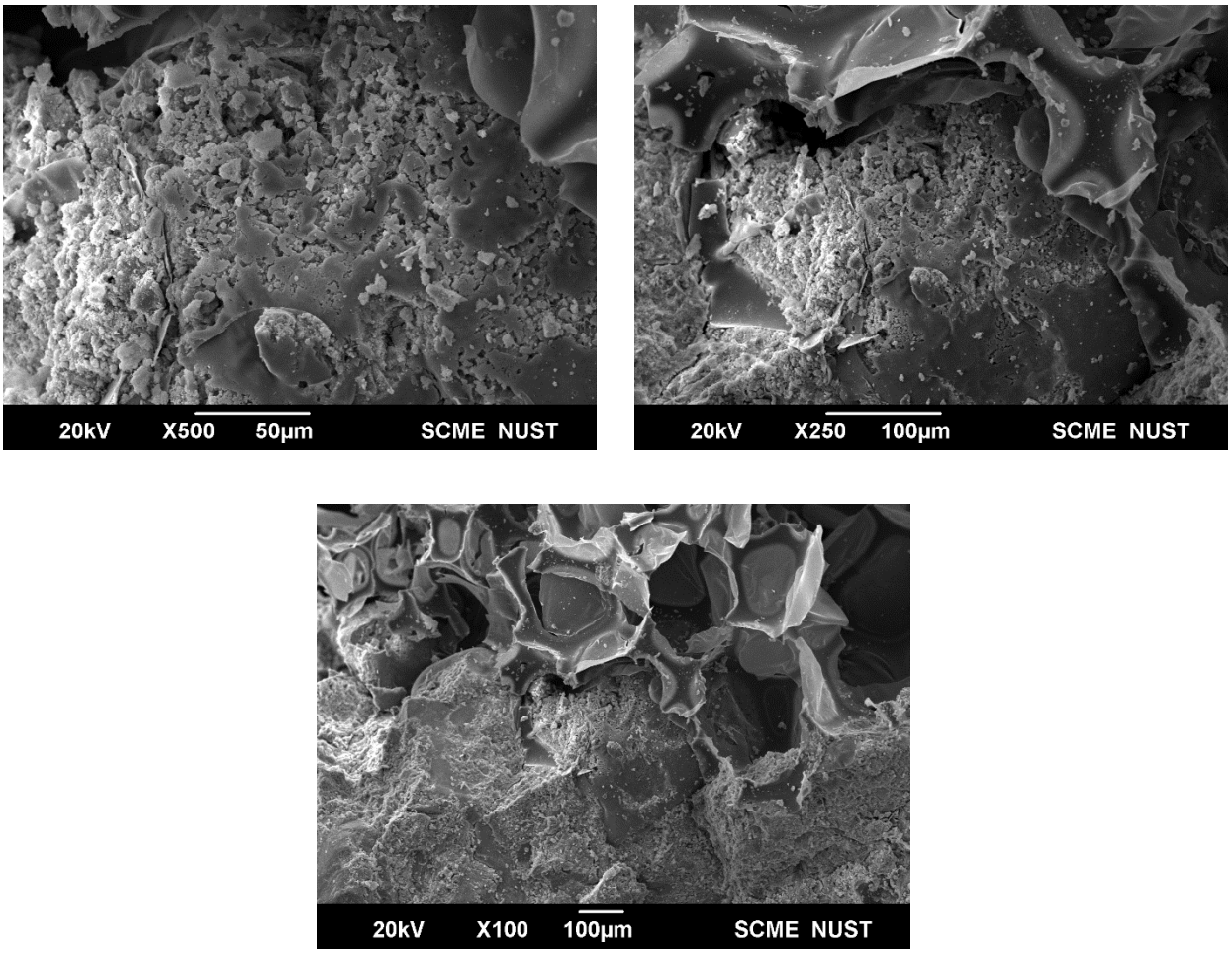

Figure 27: Interfacial zone micrographs by SEM at 28-days between the cementitious matrix and Polyurethane foam (A mix)

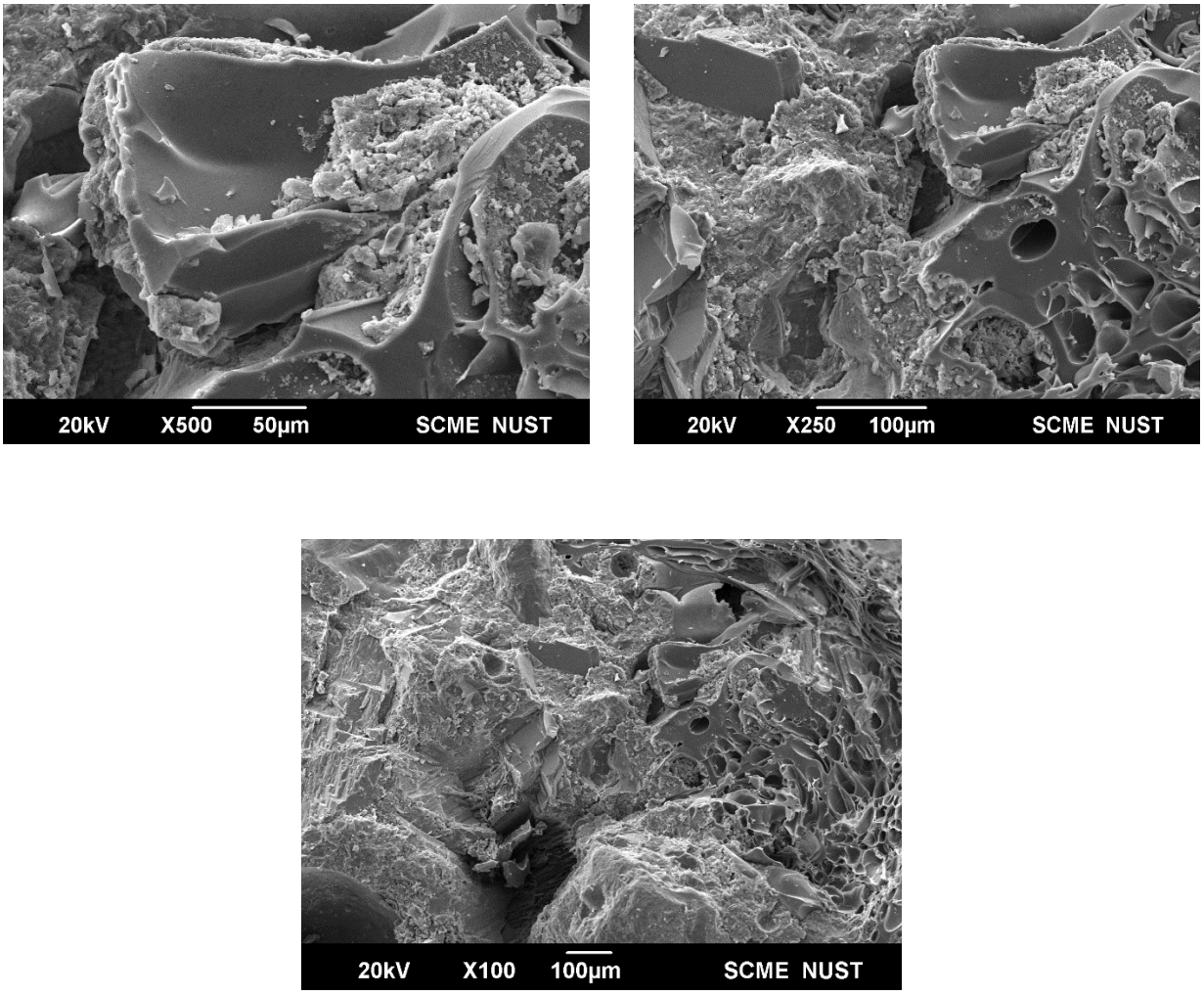

Figure 28: Interfacial zone micrographs by SEM at 28-days between the cementitious matrix and pumice aggregates (C mix)

5.10.1 Energy Dispersive X-ray Analysis (EDX)

Microstructure of the PUR-foam based LWC and Pumice based LWC are depicted in Figure 29 and 30, respectively. The elemental percentages of both the concretes are tabulated in Table 25 and 26.

Scanning electron microscopy (SEM) was utilized to analyze the produced concrete microstructure. Since both the PU foam and pumice are chemically inert, comparisons of the elemental percentages of the PU-based LWAC and the pumice-based LWAC revealed that the elemental percentages were quite comparable

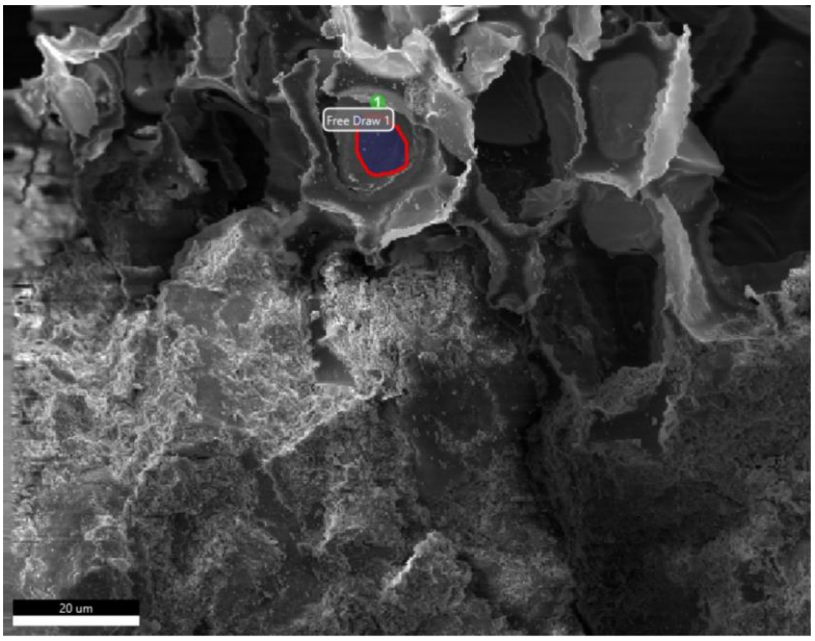

Figure 29: SEM micrograph of PUR-foam based LWC at 28-days (A mix)

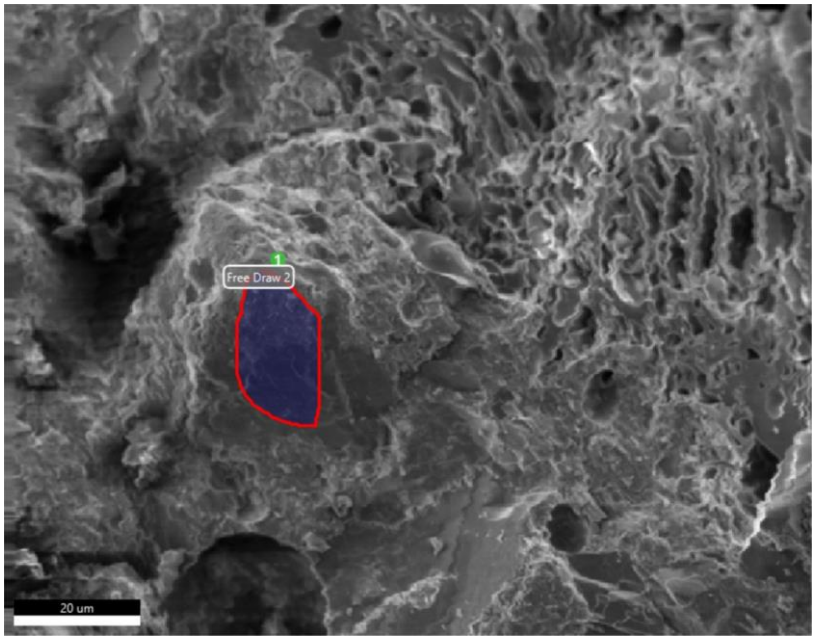

Figure 30: SEM micrograph of Pumice-based LWC at 28-days (C mix)

Although the border widths and pore size distribution were not uniform, PU-based LWAC demonstrated a dense microstructure in the borders. In this study, a water to cement ratio of 0.45 was utilized in the production process. Better homogeneity may be achieved with further concrete optimization.

Table 25: EDX Analysis Results of PUR-foam based LWC

Element	Weight (%)
O	46.6
Na	1.5
Mg	0.8
Al	1.5
Si	5.3
S	23.2
K	0.5
Ca	19.0
Fe	1.7

Table 26: EDX Analysis Results of pumice-based LWC

Element	Weight (%)
O	33.3
Na	4.0
Mg	0.6
Al	10.1
Si	11.0
S	23.7
K	1.0
Ca	15.0
Fe	1.3

CHAPTER 6: ANALYSIS OF RESULTS

6.1 Material Cost Analysis

The material cost of PU-based LWAC is compared to the material cost of conventional R.C.C to construct a double story frame structure (beams and columns) with the following dimensions to ascertain its financial viability for construction:

- Beam cross-section size = 12' x 12'
- Column cross-section size = 12' x 12'

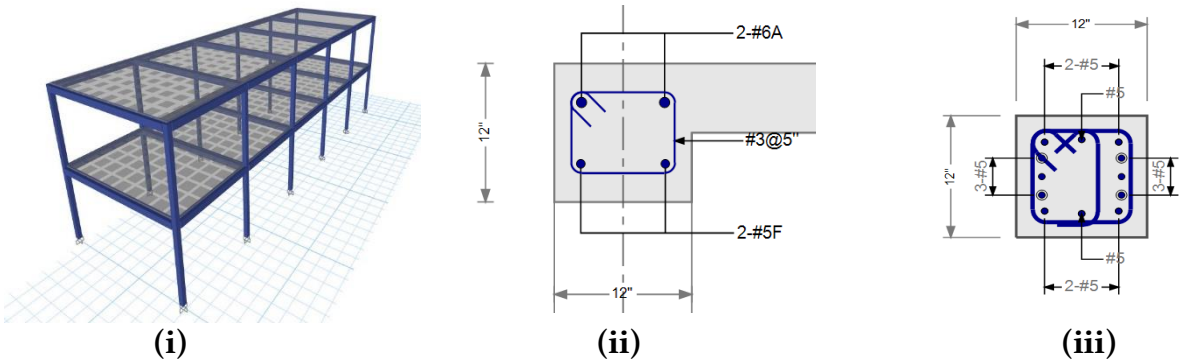

(i) (ii) (iii)

Figure 31: (i) Isometric View (ii) Beam Cross-section (iii) Column Cross-section

Table 27: Conventional Concrete Material Cost (Rates in PKR)

Conventional Concrete				
Material	**Quantity**	**Bags**	**Rate**	**Cost**
Cement	6678.08 kg	134	860/bag	115240
Sand	561.376 ft^3	-	90/ ft^3	50523.831
Normal Weight Aggregate	551.985 ft^3	-	130/ ft^3	71758.03
Steel Reinforcement	9.915 ton	-	235000/ton	2330025
Total Cost				2,567,547

Table 28: PU-based LWC Material Cost (Rates in PKR)

PU-based Concrete				
Material	**Quantity**	**Bags**	**Rate**	**Cost**
Cement	13992.92 kg	280	860/kg	240800
Sand	869.706 ft^3	-	90/ ft^3	78273.54
Polyurethane Waste	200 kg	-	50/kg	10000
Silica Fume	2372.22 kg	-	45/kg	106749.9
Steel Reinforcement	8.056 ton	-	235000/ton	1893160
Total Cost				2,328,983

Table 29: Summary of Material Cost for the Two Cases

Type of Construction	**Cost (Rs.)**	**% Difference**
PU-LWC frame structure	2,328,983	-
R.C.C frame structure	2,567,547	9.3% expensive

The summary of the cost analysis is detailed in Table 29, and it reveals that the material cost for PU-based LWAC is 9.3% less than that of conventional normal weight concrete, making it a great substitute for conventional building technologies, without significantly increasing cost.

CHAPTER 7: CONCLUSIONS AND RECOMMENDATIONS

7.1 Conclusions

1) It has been demonstrated PUR foam waste can be used to make structural lightweight aggregate concrete. When pre-coated PUR-foam aggregates were used, these concretes demonstrated less absorption and drying shrinkage.

2) Using PUR foam LWA produce more porous concretes, allowing for moisture exchange with the environment and increasing drying shrinkage, permeable voids, and penetration of chloride ion under saturated conditions.

3) The compressive strength and modulus of elasticity of the PU-based LWC varies between 13 to 19.5 MPa and 6.98 to 12.52 GPa, respectively. The corresponding air-dry density was found to be 1666 to 1829 kg/m^3. Concrete made with PUR foam LWA, met the structural LWAC requirements, however, concrete manufactured with pre coated PU foam failed to meet the criteria of LWAC thus not suitable for structural purposes.

4) The flexural strength varies from 2.33 to 2.78 MPa. Elastic and rupture modulus of concrete manufactured with uncoated PU foam are also in agreement with the criteria of ACI 213R.

5) Silica fume is optimized at 10% that is giving maximum strength. Drying Shrinkage with and without silica fume is almost equal.

6) Concrete with PU foam as an aggregate is performing better against frost action and providing good thermal properties.

7) Utilizing these “low cost” lightweight aggregates help to lower the cost per unit volume of lightweight aggregate concrete.

7.2 Recommendations

1) Seismic Analysis of PU foam based LWAC

2) Assessing the behavior of PU-based LWAC under creep, fatigue and cycling loading

3) The experimental and analytical studies on the long-term behavior of PU based concrete beams in flexure that take shrinkage and creep into account
4) Analyze the response of reinforced concrete sections
5) Analyze the stress-strain relationship of PU-based LWAC.
6) Detailed thermal analysis of PU-based concrete structure
7) Testing PU-based LWAC structure for Fire Rating

REFERENCES

[1] Hjh Kamsiah, M., Mohamad, S., & Norpadzlihatum bte, M. (1997). First report research project on lightweight concrete. 71908(2), 35–43. [CrossRef]

[2] Jagtap, P. J., Rathod, M. R., Shahebaz, S., & Murtuja, S. (2020). A Review Paper on Comparative Study of Lightweight Concrete and Reinforced Concrete. International Research Journal of Engineering and Technology, 7(3), 2616–2620. [CrossRef]

[3] Zevenhoven R. Treatment and disposal of polyurethane wastes: options for recovery and recycling. Report TKK-ENY-19, Helsinki University of Technology, Department of Mechanical Engineering, Energy Engineering and Environmental Protection Publications; 2004. [CrossRef]

[4] Mounanga, P., Gbongbon, W., Poullain, P., & Turcry, P. (2008). Proportioning and characterization of lightweight concrete mixtures made with rigid polyurethane foam wastes. Cement and Concrete Composites, 30(9), 806–814. [CrossRef]

[5] J. Yi, M.C. Boyce, G.F. Lee, E. Balizer, Large deformation rate dependent stress-strain behavior of polyurea and polyurethanes, Polymer 47 (2006) 319–329. [CrossRef]

[6] S. Chen, Q. Wang, T. Wang, Damping, thermal, and mechanical properties of carbon nanotubes modified castor oil-based polyurethane/epoxy interpenetrating polymer network composites, Mater. Des. 38 (2012) 47–52. [CrossRef]

[7] Mehta, A., & Ashish, D. K. (2020). Silica fume and waste glass in cement concrete production: A review. Journal of Building Engineering, 29, 100888. [CrossRef]

[8] Ahmad, S., Baghabra Al-Amoudi, O. S., Khan, S. M. S., & Maslehuddin, M. (2022). Effect of silica fume inclusion on the strength, shrinkage and durability characteristics of natural pozzolan-based cement concrete. Case Studies in Construction Materials, 17, e01255. [CrossRef]

[9] Kadri, El-Hadj & Duval, Roger & Aggoun, Salima & Kenai, S.. (2009). Silica Fume Effect on Hydration Heat and Compressive Strength of High-Performance Concrete. ACI Materials Journal. 106. 107-113. [CrossRef]

[10] Ali, F. M., & Mohaisen, J. M. (2019). Available online www.jsaer.com Research Article Production of Lightweight Concrete with renewable polyurethane Foam as Coarse Aggregate. 6(7), 131–137. [CrossRef]

[11] Dvorský, T., Dirner, V., Daxner, J., & Martin, Š. (n.d.). POLYURETHANE FOAM AS AGGREGATE FOR THERMAL INSULATING MORTARS AND. 665–672. [CrossRef]

[12] Ben Fraj, A., Kismi, M., & Mounanga, P. (2010). Valorization of coarse rigid polyurethane foam waste in lightweight aggregate concrete. Construction and Building Materials, 24(6), 1069–1077. [CrossRef]

[13] Harith, I. K. (2018). Study on polyurethane foamed concrete for use in structural applications. Case Studies in Construction Materials, 8, 79–86. [CrossRef]

[14] Babu, K. G., & Babu, D. S. (2003). Behaviour of lightweight expanded polystyrene concrete containing silica fume. Cement and Concrete Research, 33(5), 755–762. [CrossRef]

[15] Giner, V. T., Ivorra, S., Baeza, F. J., Zornoza, E., & Ferrer, B. (2011). Silica fume admixture effect on the dynamic properties of concrete. Construction and Building Materials, 25(8), 3272–3277. [CrossRef]

[16] Amudhavalli, N. K., & Mathew, J. (2012). Effect of Silica Fume on Strength and Durability Parameters of Concrete. International Journal of Engineering Sciences & Emerging Technologies, 3(1), 2231–6604. [CrossRef]

[17] H. Katkhuda, B. Hanayneh, & N. Shatarat. (2009). Influence of SF in LFC. 781–788. [CrossRef]

[18] Kumar, D., Roy, S., & Sil, A. (2012). International Journal of Emerging Technology and Advanced Engineering Effect of Partial Replacement of Cement by Silica Fume on Hardened Concrete. 2(8), 472–475. [CrossRef]

[19] ASTM C150/C150M-20, Standard Specification for Portland Cement. In ASTM Volume 04.01 Cement; Lime; Gypsum; ASTM International: West Conshohocken, PA, USA, 1999; pp. 1–9. ISBN 591988l100 [CrossRef]

[20] ASTM C 1240. (2005). Standard Specification for Silica Fume Used in Cementitious Mixtures. ASTM International, 15, 1–7. [CrossRef]

[21] ASTM C494/C494M-08a Standard Specification for Chemical Admixtures for Concrete. In ASTM Volume 04.02 Concrete and Aggregates; ASTM International: West Conshohocken, PA, USA, 2014; pp. 1–10 [CrossRef]

[22] ASTM. Standard test method for sieve analysis of fine aggregates, C 136–01. In: Bailey SJ, Baldini NC, McElrone EK, Peters KA, Rosiak JL, Simms ST, Terruso DA, Whealen EA, editors. Annual Book of ASTM Standards Concrete and Aggregates, 2004; vol. 4. No. 4.02. p. 84–8 [CrossRef]

[23] ASTM. Specifications for concrete aggregates, C 33-03. In: Bailey SJ, Baldini NC, McElrone EK, Peters KA, Rosiak JL, Simms ST, Terruso DA, Whealen EA, editors. Annual Book of ASTM Standards Concrete and Aggregates, 2004; vol. 4. No. 4.02. p. 10–20. [CrossRef]

[24] ASTM C192 / C192M-19, Standard Practice for Making and Curing Concrete Test Specimens in the Laboratory, ASTM International, West Conshohocken, PA, 2019 [Cross Ref]

[25] ASTM C511-19 Standard Specification for Mixing Rooms, Moist Cabinets, Moist Rooms, and Water Storage Tanks Used in the Testing of Hydraulic Cements and Concretes. In ASTM Standard Guide; ASTM International: West Conshohocken, PA, USA, 2015; pp. 23–25. [CrossRef]

[26] ASTM C330. (2009). Standard Specification for Lightweight Aggregates for Structural Concrete. ASTM International, 552(18), 4. [CrossRef]

[27] ASTM C143/C143M-12, Standard Test Method for Slump of Hydraulic cement concrete. ASTM International Vol 04.02. [CrossRef]

[28] ASTM C138/C138M-17a. Standard Test Method for Density (Unit Weight), Yield , and Air Content (Gravimetric) of concrete. 1–6. [CrossRef]

[29] ASTM C642-21. Standard Test Method for Density , Absorption , and Voids in Hardened Concrete. March, 1–3. [CrossRef]

[30] ASTM C293/C293M-08. ASTM Standards C 293-02. Standard Test Method for Flexural Strength of Concrete (Using Simple Beam With Center-Point Loading), 1–3. [CrossRef]

[31] ASTM C39-14. Standard Test Method for Compressive Strength of Cylindrical Concrete Specimens. ASTM Standard Book, i(March), 1–5. [CrossRef]

[32] ASTM C469-02. Standard Test Method for Static Modulus of Elasticity and Poisson ' s Ratio of Concrete. 04, 1–5. [CrossRef]

[33] ASTM C596-18, Standard Test Method for Drying Shrinkage of Mortar Containing Hydraulic Cement, ASTM International, West Conshohocken, PA, 2018 [CrossRef]

[34] Layssi, Hamed & Ghods, Pouria & Alizadeh, Aali & Salehi, Mustafa. (2015). Electrical Resistivity of Concrete. Concrete International. 37. 41-46. [CrossRef]

[35] ASTM C1202-19, Standard Test Method for Electrical Indication of Concrete's Ability to Resist Chloride Ion Penetration, ASTM International, West Conshohocken, PA, 2019 [CrossRef]

[36] AASHTO TP95-11. (2015). Evaluation of Surface Resistivity Indication of Ability of Concrete to Resist Chloride Ion Penetration. New Jersey Department of Transportation, 1(March), 1–9. [CrossRef]

[37] Bao Lu, ... Tung-Chai Ling, in Carbon Dioxide Sequestration in Cementitious Construction Materials, 2018 [CrossRef]

[38] Pospíchal, O., Kucharczyková, B., Misák, P., & Vymazal, T. (2010). Freeze-thaw resistance of concrete with porous aggregate. Procedia Engineering, 2(1), 521–529. [CrossRef]

[39] Mao, Jize & Ayuta, Koichi. (2008). Freeze–Thaw Resistance of Lightweight Concrete and Aggregate at Different Freezing Rates. Journal of Materials in Civil Engineering - J MATER CIVIL ENG. 20. 10.1061/(ASCE)0899-1561(2008)20:1(78). [CrossRef]

[40] BSI PD CEN/TR 15177:2006 Testing the freeze-thaw resistance of concrete-Internal structural damage. [CrossRef]

[41] ASTM E1530-99, Standard Test Method for Evaluating the Resistance to Thermal Transmission of Thin Specimens of Materials by the Guarded Heat Flow Meter Technique, ASTM International, West Conshohocken, PA, 1999 [CrossRef]

[42] Mazloom, M., Ramezanianpour, A. A., & Brooks, J. J. (2004). Effect of silica fume on mechanical properties of high-strength concrete. Cement and Concrete Composites, 26(4), 347–357. [CrossRef]

[43] Neville AM. Properties of concrete. 4th ed. Essex (England): Addison Wesley Longman; 1997. [CrossRef]

[44] Al-Khaiat H, Haque MN. Effect of initial curing on early strength and physical properties of a lightweight concrete. Cem Concr Res 1998;28(6):859–66. [CrossRef]

[45] Chi JM, Huang R, Yang CC, Chang JJ. Effect of aggregate properties on the strength and stiffness of lightweight concrete. Cem Concr Compos 2003;25(2):197–205. [CrossRef]

[46] Saradhi Babu D, Ganesh Babu K, Wee TH. Effect of polystyrene aggregate size on strength and moisture migration characteristics of lightweight concrete. Cem Concr Compos 2006;28(6):520–7. [CrossRef]

[47] Torres ML, García-Ruiz PA. Lightweight pozzolanic materials used in mortars: evaluation of their influence on density, mechanical strength and water absorption. Cem Concr Compos 2009;31(2):114–9. [CrossRef]

[48] Thomas, Telford. State of Art Report, Condensed Silica Fume in Concrete, FIP Commission on Concrete, 1988. [CrossRef]

[49] Wang, Xiao-Yong. (2014). Effect of fly ash on properties evolution of cement based materials. Construction and Building Materials. 69. 32–40. [CrossRef]

[50] Kondraivendhan, Ba & Bhattacharjee, Bishwajit. (2015). Flow behavior and strength for fly ash blended cement paste and mortar. International Journal of Sustainable Built Environment. 14. [CrossRef]

[51] ACI 213R-14 (2014). Guide for Structural Lightweight Aggregate Concrete. (Reapproved), 1–27. [CrossRef]

[52] Kayali O. Fly ash lightweight aggregates in high performance concrete. Constr Build Mater 2008;22(12):2393–9. [CrossRef]

[53] Aamr-Daya E, Langlet T, Benazzouk A, Quéneudec M. Feasibility study of lightweight cement composite containing flax by-product particles: physicomechanical properties. Cem Concr Compos 2008;30(10):957–63. [CrossRef]

[54] Siddique R, Khatib J, Kaur I. Use of recycled plastic in concrete: a review. Waste Manage 2008;28(10):1835–52. [CrossRef]

[55] Saradhi Babu D, Ganesh Babu K, Wee TH. Effect of polystyrene aggregate size on strength and moisture migration characteristics of lightweight concrete. Cem Concr Compos 2006;28(6):520–7 [CrossRef]

[56] Chia KS, Zhang M-H. Water permeability and chloride penetrability of highstrength lightweight aggregate concrete. Cem Concr Res 2002;32(4):639-45. [CrossRef]

[57] Kohno K, Okamoto T, Isikawa Y, Sibata T, Mori H. Effects of artificial lightweight aggregate on autogenous shrinkage of concrete. Cem Concr Res 1999;29(4):611–4. [CrossRef]

[58] Ding Q, Tian Y, Wang F, Zhang F, Hu S. Autogenous shrinkage of high strength lightweight aggregate concrete. J Wuhan Univ Technol 2005;20:123–5. [CrossRef]

[59] Mounanga P, Baroghel-Bouny V, Khelidj A, Loukili A. Autogenous deformations of cement pastes—part I: temperature effects at early age and micro–macro correlations. Cem Concr Res 2006;36(1):110–22. [CrossRef]

[60] ASTM C157 / C157M-17, Standard Test Method for Length Change of Hardened Hydraulic-Cement Mortar and Concrete, ASTM International, West Conshohocken, PA, 2017. [CrossRef]

[61] AS 3972-2010 General purpose and blended cements. [CrossRef]

[62] Chen B, Liu J. Properties of lightweight expanded polystyrene concrete reinforced with steel fiber. Cem Concr Res 2004;34(7):1259–63. [CrossRef]

[63] Hossain KMA. Properties of volcanic pumice based cement and lightweight concrete. Cem Concr Res 2004;34(2):283–91. [CrossRef]

[64] Alduaij J, Alshaleh K, Haque MN, Ellaithy K. Lightweight concrete in hot coastal areas. Cem Concr Compos 1999;21(5–6):453–8. [CrossRef]

[65] Brooks, J. J and Neville, A.M. A Comparison of Creep, Elasticity and Strength of Concrete in Tension and in Compression. Magazine of Concrete Research, V. 29, No.100, pp. 131-141, 1977. [CrossRef]

[66] El-Hindy, E., Miao, B.Q., Chaalla, O. and Aitcin, P.C., Drying Shrinkage of Ready Mixed High-Performance Concrete, ACI Material Journals, V.63, No.63, pp. 111-116, 1994. [CrossRef]

[67] Carrete, G.G. and Malhotra, V.M., Mechanism Properties, Durability and Drying Shrinkage of Portland Cement Concrete Incorporating Silica Fume. Cement Concrete and Aggregates V. 5, No.1, pp 3-13, 1983 [CrossRef]

[68] Sugair, F.H. Analysis of the Time –Dependent Volume Reduction of Concrete Containing Silica Fume. Magazine of Concrete Research, V. 47, No.170, pp. 78-81, 1995. [CrossRef]

[69] Zhang M-H, Gjørv OE. Permeability of high strength lightweight concrete. ACI Mater J 1991;88:463–9. [CrossRef]

[70] Sugiyama T, Bremner TW, Tsuji Y. Determination of chloride diffusion coefficient and gas permeability of concrete and their relationship. Cem Concr Res 1996;26(5):781–90. [CrossRef]

[71] Shafigh, P.; Asadi, I.; Akhiani, A.R.; Mahyuddin, N.B.; Hashemi, M. (2020) Thermal properties of cement mortar with different mix proportions. Mater. Construcc. 70 [339], e224. [CrossRef]

[72] Shi, Jinyan & Liu, Yuanchun & Liu, Baoju & Han, Dan. (2019). Temperature Effect on the Thermal Conductivity of Expanded Polystyrene Foamed Concrete: Experimental Investigation and Model Correction. Advances in Materials Science and Engineering. 2019. 1-9. [CrossRef]

[73] Demirboğa, R., & Gül, R. (2004). Durability of mineral admixtured lightweight aggregate concrete. In Indian Journal of Engineering & Materials Sciences (Vol. 11). [CrossRef]

[74] Zhou Y, Cohen M & Dolch W L, ACI Mater J, 91 (1994) 595-601. [CrossRef]

[75] Ollivier JP, Maso JC, Bourdette B. Interfacial transition zone in concrete. Adv Cem Based Mater 1995;2(1):30–8. [CrossRef]

[76] Kayali O. Fly ash lightweight aggregates in high performance concrete. Constr Build Mater 2008;22(12):2393–9. [CrossRef]

[77] Zhang M-H, Gjørv OE. Microstructure of the interfacial zone between lightweight aggregate and cement paste. Cem Concr Res 1990;20(4):610–8. [CrossRef]

[78] Lo TY, Cui HZ. Effect of porous lightweight aggregate on strength of concrete. Mater Lett 2004;58(6):916–9. [CrossRef]